FACTORS THAT INFLUENCE MAMMALIAN ENTERIC VIRUS INFECTION

APPROVED BY SUPERVISORY COMMITTEE

_____

John Schoggins, Ph.D. Chair

_____

Julie Pfeiffer, Ph.D.

_____

Tiffany Reese, Ph.D.

_____

Sebastian Winter, Ph.D.

FACTORS THAT INFLUENCE MAMMALIAN ENTERIC VIRUS INFECTION

by

ELIZABETH RENATA AGUILERA

DISSERTATION

Presented to the Faculty of the Graduate School of Biomedical Sciences

The University of Texas Southwestern Medical Center at Dallas

In Partial Fulfillment of the Requirements

For the Degree of

DOCTOR OF PHILOSOPHY

The University of Texas Southwestern Medical Center at Dallas

Dallas, Texas

DEDICATION

To my little family, Zachary and Milo.

ACKNOWLEDGEMENTS

I would first and foremost like to thank Julie for being the best mentor that I could ask for during my dissertation research. I am grateful for Julie's patience and guidance throughout my time in her lab. Julie is an inspiration and I can only hope that I can be as great of a scientist and mentor as her.

I would also like to thank my committee members John, Tiffany and Sebastian for their support, recommendations and advice.

I also want to thank the members of the Pfeiffer lab (past and present) for the great memories throughout the years. Thank you to Andrea, Chris, Palmy, Lauren, Yao, Y, Broc, Arielle, Mikal and Matt for all of the advice, laughs and fun hangouts. I wish you all the best in your future scientific endeavors.

I would next like to thank my friends and family, whom I all love dearly for their encouragement along the way. I would like to thank my great friends near and far, Melissa, Lauren, and Vanessa. I also want to thank my Al-Tabbaa/Crumby family, Samir, Minerva, Adam, Jasmine, Michael and Halia. I would also like to thank my immediate family, Renato, Yolanda, Kristina and my brother-in-law Stefan for their love, guidance and support.

Finally, I would like to thank Zachary and Milo for their continuous love and support. The patience and compassion they have shown me is beyond words. I am grateful to have such a great support system, both in science and life. This dissertation would not have been possible without them.

FACTORS THAT INFLUENCE MAMMALIAN ENTERIC VIRUS INFECTION

ELIZABETH RENATA AGUILERA, Ph.D.

The University of Texas Southwestern Medical Center at Dallas, 2018

Supervising Professor: Julie K. Pfeiffer, Ph.D.

RNA viruses are a common cause of emerging diseases due to their vast genetic diversity. This diversity is largely attributed to mutations generated by the error-prone viral RNA-dependent RNA polymerase during replication. Despite the ability to acquire mutations beneficial to the virus, most mutations are deleterious and reduce viral fitness. This poses an obstacle for RNA viruses to successfully infect the host. In addition, a subset of RNA viruses are also enteric pathogens. In particular, these viruses must navigate several environments for transmission and subsequent infection through the fecal-oral route. In this work, I used poliovirus, an enteric RNA virus from the

Picornaviridae family, as a model system to study mechanisms of RNA virus co-infection and how bacteria influence picornavirus infection.

Recent studies determined several modes of RNA virus transmission exist outside of canonical pathways, including en bloc transmission of multiple viruses into a single cell via bacteria or host-derived membrane vesicles. Co-infection of RNA viruses is important since it can enhance viral fitness. I determined that multiple polioviruses are found within a single plaque even at low multiplicity of infection. I also showed that poliovirus stocks contain virion aggregates and that aggregates induce co-infection. Furthermore, I found that co-infection frequency was increased when polioviruses were heavily mutagenized. This work suggests that co-infection can contribute to plaque formation and that co-infection may assist plaque formation in situations with high genomic damage. This work contributes to mechanisms that influence co-infection of RNA viruses and potentially drive viral evolution.

Infection by members of the *Picornaviridae* family can cause respiratory, cardiac, gastrointestinal, and neurological disease. These and other viruses encounter various bacteria within the host and in the environment. Despite these close encounters, the effects of bacteria on picornaviruses is not completely understood. Previous work determined that poliovirus has enhanced virion stability when exposed to bacteria or bacterial polysaccharides. Therefore, I investigated whether bacteria broadly enhance stability of picornaviruses from three different genera: *Enterovirus* (PV and coxsackievirus B3 (CVB3)), *Kobuvirus* (Aichi virus) and *Cardiovirus* (Mengo virus). I determined that specific bacterial strains enhance thermal stability of subset of viruses, while others were stable in the absence of bacteria. Additionally, I determined that bacteria can stabilize the

entire picornavirus panel when individually exposed to bleach. These effects are likely mediated through direct interactions with bacteria since viruses bound to bacteria *in vitro*. Overall, this work reveals shared and distinct effects of bacteria on a panel of picornaviruses with implications on viral transmission.

TABLE OF CONTENTS

PRIOR PUBLICATIONS

Aguilera ER, Erickson AK, Jesudhasan PR, Robinson CM, Pfeiffer JK. 2017. Plaques formed by mutagenized viral populations have elevated coinfection frequencies. *mBio* 8:e02020-16. https://doi.org/10.1128/mBio.02020-16.

Aguilera ER, Nguyen Y, Sasaki J, Pfeiffer JK. 2018. Bacteria-mediated stabilization of a panel of picornaviruses. (manuscript submitted, *Journal of Virology*).

Aguilera ER and Pfeiffer JK. 2018. Strength in numbers: mechanisms of viral co-infection. (manuscript submitted, *Journal of Virology*).

Nguyen Y, Jesudhasan PR, **Aguilera ER**, Pfeiffer JK. 2018. Characterization of a thermal stable poliovirus mutant reveals distinct mechanisms of virion stabilization. (manuscript submitted, *Virus Research*).

Dong X, Yang Y, Zou Z, Ci B, **Aguilera ER**, Richardson B, Xavier R, Schoggins JW, Pfeiffer JK, Gleeson PA, Ktistakis NT, Cullen PJ, Xiao G, Levine B. 2018. Sorting Nexin 5 as a Novel Mediator of Virus-Induced Autophagy and Antiviral Immunity. (manuscript in preparation)

LIST OF FIGURES

LIST OF TABLES

ABBREVIATIONS

AMP – antimicrobial peptide

BSA – bovine albumin serum

CAR – coxsackievirus and adenovirus receptor

CVB3 – coxsackievirus B3

DAF – decay-accelerating growth factor

dpi – days post infection

DsRED – *Discosoma sp*. red fluorescent protein

EMCV – encephalomyocarditis virus

GFP – green fluorescent protein

GlcNAc – N-acetylglucosamine

HBGA – histo-blood group antigen

hpi – hours post infection

HS – heparan sulfate

IEC – intestinal epithelial cell

IFN – interferon

IFNAR – interferon-alpha/beta receptor

LPS – lipopolysaccharide

MOI – multiplicity of infection

MMTV – mouse mammary tumor virus

OPV – oral poliovirus vaccine

PBS – phosphate buffered saline

PFU – plaque forming unit

PG – peptidoglycan

PV – poliovirus

PVR – poliovirus receptor

PVRtg – poliovirus receptor transgene

RBV – ribavirin

RdRp – RNA dependent RNA polymerase

RNA – ribonucleic acid

VCAM-1 – vascular cell adhesion molecule-1

VDPV – vaccine-derived poliovirus

WT – wild-type

CHAPTER ONE

Introduction

RNA Viruses

RNA viruses are a major global threat to the human population. Of particular medical relevance are the human immunodeficiency virus and influenza viruses, to name a few. Viruses containing RNA genomes can readily adapt to specific selective pressures due to their highly diverse viral population. This diversity is largely attributed to error-prone replication of RNA viruses that results in the acquisition of mutations in the viral genome. These and other factors contribute to the pathogenicity, adaptability and evolution of RNA viruses. The study of RNA viruses and the factors that influence infection are pertinent to develop an in-depth understanding of viral transmission and evolution.

The *Picornaviridae* Family

The *Picornaviridae* viral family is composed of over 80 species that span over 35 genera. The family name describes the small (pico-) RNA-containing viruses (Fields Virology, 2013). Members of this family are non-enveloped and contain a single-stranded, positive sense RNA genome approximately 7,500 nucleotides in length. Generally, the RNA genome is enclosed within an icosahedral capsid composed of 60 copies each of four structural proteins: VP1, VP2, VP3 and VP4. VP1, VP2 and VP3 are surface exposed, while VP4 is predominantly internal. One copy of each structural protein constitute the capsid protomer. Five copies of the protomer constitute a pentamer, which surrounds a fivefold axis of symmetry on the surface of the virion For several picornaviruses, this axis is surrounded by a canyon which varies in topological depth and

is dependent on the viral species. At the base of the canyon lies a hydrophobic pocket found in most picornaviruses. This pocket is occupied by a lipid “pocket factor” that is released during the uncoating process. The canyon plays an important role in viral receptor engagement and entry for several picornaviruses (Fields Virology, 2013).

Upon attachment of the picornavirus to its cognate viral receptor, and possibly coreceptor(s), the virion undergoes conformational changes required for entry. The viral genome is subsequently released into the host cell cytoplasm and recruits host cell ribosomes for viral protein translation. As positive-stranded viruses, RNA translation immediately occurs and generates the viral polyprotein. The viral polyprotein is cleaved by the viral proteases to generate the structural and nonstructural proteins required for formation of the capsid and replication machinery, respectively. After replication, the virus exits the cell through lytic and non-lytic mechanisms (Fields Virology, 2013).

Poliovirus

Poliovirus was first identified in 1909 as the causative agent of acute flaccid paralysis, known as poliomyelitis (Landsteiner and Popper, 1909). In infected humans, poliovirus can be shed in feces 2-8 weeks post-infection (Racaniello, 2006). Poliomyelitis only occurs when poliovirus enters the central nervous system followed by infection and damage of motor neurons. Despite this hallmark disease, poliovirus causes paralysis in less than 1% of infected individuals. Due to the global initiative to eradicate the disease through vaccination measures, cases of poliovirus have decreased over 99% (Nathanson, 2008; Racaniello, 2006). Furthermore, poliovirus has been eradicated in all countries except Afghanistan, Pakistan and Nigeria. Despite this initiative, there have been several

outbreaks of vaccine-associated infections in Guinea, Madagascar and Ukraine. These specific outbreaks were caused by circulating vaccine-derived poliovirus (VDPV) and some of the infected individuals developed vaccine-associated paralytic poliomyelitis. These outbreaks are likely caused by the circulation of live, attenuated virus from the trivalent oral poliovirus vaccine (OPV) originally created by Albert Sabin (Kew et al., 2002; A. B. Sabin, 1959). There is also an inactivated poliovirus vaccine, created by Jonas Salk, that is the current vaccine used in the United States (Salk et al., 1954). VDPV can circulate in the environment because individuals who are administered the OPV are capable of shedding virus post vaccination. Additionally, outbreaks may occur through lack of available vaccines in developing countries, political unrest and vaccination refusal. These outbreaks highlight both the importance for following vaccination procedures and for understanding viral evolution.

In the laboratory, poliovirus can be used as a tool to dissect mechanisms and consequences of enteric and RNA virus infection. In particular, poliovirus can replicate in several cell types in the laboratory setting. Additionally, poliovirus has a reverse genetics system in place, suitable for generation of genetically characterized mutants (Racaniello and Baltimore, 1981). Furthermore, over 100 years of poliovirus research has yielded a large set of previously characterized and readily available mutants with various phenotypes (Leveque and Semler, 2015; Racaniello, 2006).

Poliovirus is a member of the *Picornaviridae* family and is spread through the fecal-oral route. Three serotypes of poliovirus exist, type 1 (Mahoney), type 2 (Lansing) and type 3 (Leon), and serotype is determined by the viral capsid. Poliovirus type 1 is the predominant strain circulating within the human population. Poliovirus type 1 has been

extensively studied which has led to the generation and characterization of several mutants. In this dissertation, poliovirus type 1 is the predominant strain used in the studies described.

Although the main cell target of poliovirus in the gastrointestinal tract is unknown, poliovirus infection occurs within cells expressing the poliovirus receptor (PVR), or CD155 (C. Mendelsohn et al., 1986; C. L. Mendelsohn et al., 1989). PVR was identified as a member of the immunoglobulin superfamily (C. Mendelsohn et al., 1986; C. L. Mendelsohn et al., 1989). Within the intestine, poliovirus may infect epithelial Microfold (M) cells (Ouzilou et al., 2002; Sicinski et al., 1990). The PVR is ubiquitously expressed in nearly all human cells and is used by all three serotypes of poliovirus. Apart from expression in humans, PVR has homologs in Old World Primates, which include chimpanzees and African green monkeys (Ida-Hosonuma et al., 2003). However, conventional mice do not express human PVR and are not susceptible to infection by poliovirus. Once the cognate receptor for poliovirus was identified, a PVR transgenic (PVRtg) mouse model was generated to study viral pathogenesis (C. Mendelsohn et al., 1986; R. B. Ren et al., 1990). In PVRtg mice, PVR is expressed in nearly all tissues, including the intestine (Koike et al., 1991; R. Ren and Racaniello, 1992; R. B. Ren et al., 1990). These mice are susceptible to all 3 poliovirus serotypes. Additionally, these mice express PVR in most tissues, but disease does not occur following oral inoculation of poliovirus. However, poliovirus is pathogenic to PVRtg mice following intramuscular, intraspinal, intracerebral and intraperitoneal injection (Koike et al., 1991; R. Ren and Racaniello, 1992; R. B. Ren et al., 1990). Although PVR is widely expressed, not all tissues are infected by poliovirus, suggesting that PVR is not the sole determinant of

tissue tropism for poliovirus. Since picornaviruses were previously shown to be sensitive to the type 1 interferon response, mice were generated that express PVR, but lack expression of the interferon α/β receptor (PVRtg-IFNAR -/-) (Chebath et al., 1987; Ida-Hosonuma et al., 2005; Ohka et al., 2007). Knockout of the IFN α/β receptor renders the mouse incapable of responding to interferon, a molecule essential in the innate immune response to various pathogens, including viruses. Importantly, PVRtg-IFNAR -/- mice are susceptible to poliovirus after oral inoculation (Ida-Hosonuma et al., 2005; Ohka et al., 2007). This study was the first to provide an oral inoculation model for poliovirus infection, which is the natural route of infection (Ida-Hosonuma et al., 2005; Ohka et al., 2007).

Aichi virus

Aichi virus was first identified in 1989 from stool of a patient exhibiting gastroenteritis (Yamashita et al., 1991). The virus is spread through the fecal-oral route and is named after the location of the first isolation, which occurred in Aichi, Japan (Yamashita et al., 1991). Since the first isolation, Aichi has continuously been detected in stool of patients with gastroenteritis across Asia as well as in sewage in the Netherlands and elsewhere (Lodder et al., 2013; Yamashita et al., 1998). In fact, it is estimated that up to 95% of adults worldwide have been infected by Aichi virus (Kitajima and Gerba, 2015). Sequence analysis indicated the genome had approximately 20% homology to others viruses in this family and was classified into a new genus of the *Picornaviridae* family, *Kobuvirus* (Yamashita et al., 1998). A distinct characteristic of this virus from other viral family members is the formation of the mature capsid proteins. For Aichi virus, VP0 is not cleaved into the classical VP4 and VP2 capsid proteins found within other members

of this viral family (Yamashita et al., 1998). Instead, VP0 is retained in the surface-exposed protomer: VP0, VP1, VP3 (Yamashita et al., 1998). Additionally, the characteristic deep canyon observed for several other picornaviruses is subtle and shallow on the Aichi capsid surface (C. Sabin et al., 2016; Zhu et al., 2016). As previously stated, the canyon is considered an important site for virus-host receptor interactions of several picornaviruses. Intriguingly, Aichi virus also lacks the hydrophobic pocket structure of many other picornaviruses (Rossmann et al., 2002). Overall, Aichi virus has distinct topological features that differ from other members of the *Picornaviridae* family. The implications for these topological differences is still unclear.

Despite the clinical relevance of Aichi virus, mechanisms of infection and transmission are not well understood. To date, the receptor(s) remains to be identified and a mouse model for the virus is not available. However, a reverse genetics system was established for Aichi virus and this virus can replicate in Vero cells, a kidney embryonic cell line from African green monkeys (Sasaki et al., 2001).

Coxsackievirus

Coxsackievirus is a member of the *Enterovirus* genus and is transmitted through the fecal-oral route. Coxsackievirus was first identified in 1948 from stool of two patients exhibiting mild paralysis (Dalldorf and Sickles, 1948; Dalldorf et al., 1949). Indeed, this virus isolate also caused paralysis in newborn mice (Dalldorf and Sickles, 1948; Dalldorf et al., 1949). This virus is named after the location of its initial isolation: Coxsackie, New York. Coxsackieviruses are separated into two groups: Group A and Group B, which cause different pathologies in newborn mice (Dalldorf and Sickles, 1948; Dalldorf et al.,

1949; Garmaroudi et al., 2015). Group A coxsackieviruses generally cause myositis, or muscle inflammation (Bergelson et al., 1997; Garmaroudi et al., 2015). Group B viruses generally cause myocarditis, or inflammation of the heart (Garmaroudi et al., 2015). To date, 30 serotypes of coxsackievirus have been identified, 23 belonging to Group A and 6 to Group B (Garmaroudi et al., 2015). Coxsackievirus B3 (CVB3) is used in the work described in Chapter 3 of this dissertation.

CVB3 infection occurs in specific target cells expressing the coxsackievirus and adenovirus receptor (CAR), a member of the immunoglobulin family (Bergelson et al., 1997). CVB3 can also use a coreceptor, the decay-accelerating growth factor (DAF), for infection of specific cell types (Hafenstein et al., 2007; Selinka et al., 2002; Shafren et al., 1995). DAF, or CD55, is a surface-exposed regulatory protein (Hafenstein et al., 2007; Selinka et al., 2002; Shafren et al., 1995). Additionally, heparan sulfate (HS) has been implicated to be a co-receptor for coxsackieviruses (Zautner et al., 2003). Both CAR and DAF are expressed in various cells within the human host (Garmaroudi et al., 2015).

Intriguingly, sex plays an important role in CVB3 pathogenesis. In humans, males have a higher likelihood of developing disease following coxsackievirus infection when compare to females (Shah et al., 2003). Additionally, following the natural oral route of infection, males were more susceptible than females during CVB3 infection in IFNAR -/- mice (Robinson et al., 2017). Other factors, such as host bacteria, may play a role during coxsackievirus infection as germ-free mice were more susceptible than conventional mice (Schaffer et al., 1963). However, this particular finding followed infection by the intraperitoneal route, not the oral route (Schaffer et al., 1963). Indeed, studies addressing

the effects of the host gut bacteria on coxsackievirus following the natural route of infection warrant further investigation.

Mengo virus

Mengo virus belongs to the *Cardiovirus* genus and is spread through the fecal-oral route. Mengo virus was isolated in 1948 from a rhesus monkey exhibiting hind limb paralysis (Carocci and Bakkali-Kassimi, 2012; Dick et al., 1948). The virus is named after the location of initial isolation in the Mengo district of Entebbe, Uganda (Dick et al., 1948). Mengo virus is antigenically similar to another virus in the genus, encephalomyocarditis virus (EMCV). Sialoglycoproteins on human cells are involved in attachment and subsequent entry of EMCV (Burness and Pardoe, 1983). Indeed, the vascular cell adhesion molecule-1 (VCAM-1) is a sialoglycoprotein and was found to be the receptor for EMCV on primary murine vascular endothelial cells (Huber, 1994). However, the exact cell receptor(s) for Mengo virus in human cell lines are still unknown.

While EMCV and Mengo viruses rarely cause disease in humans, these viruses can infect a multitude of hosts. In non-human primates, these viruses can cause acute heart failure (Carocci and Bakkali-Kassimi, 2012). In mammals, such as pigs and mice, these viruses can cause myocarditis (Carocci and Bakkali-Kassimi, 2012). Furthermore, EMCV and Mengo virus can cause meningo-encephalomyelitis in mice infected by intraperitoneal or intracerebral routes (Veckenstedt, 1974). Many mouse strains are susceptible to EMCV and Mengo virus infection, however studies utilizing these models often bypass the natural fecal-oral route of infection. Indeed, studies of Mengo virus by

oral inoculation have not been performed and the factors that may facilitate infection by this route are unknown.

RNA VIRUS QUASISPECIES THEORY AND VIRAL EVOLUTION

RNA viruses, including poliovirus, are genetically diverse. RNA viruses harbor various mutations in their genome due to the lack of proofreading activity of the viral RNA dependent RNA polymerase (RdRp). RNA viral genomes can contain an average of one mutation per genome due to this mechanism alone (Domingo and Holland, 1997; Drake, 1993). Like many other RNA viruses, poliovirus has a high particle to plaque forming unit (PFU) ratio: 30:1 to 1,000:1 due to assembly defects, mutations and inefficient cell attachment (Fields Virology, 2013). For poliovirus, the mutation frequency is approximately 10^{-4} per nucleotide, per replication cycle *in vitro* (Ward et al., 1988). This mutation frequency generates heterogeneous viruses within a population, also commonly referred to as a viral quasispecies (Domingo et al., 1985). The theory of quasispecies is a mathematical concept to describe complex populations and has been applied to RNA virus populations (Domingo et al., 1985) .

Diverse populations of viruses carrying unique mutations can be beneficial to the virus by conferring resistance to neutralizing antibodies or drug treatments. However, most mutations are detrimental and reduce fitness of the virus. Intriguingly, passage of poliovirus in the presence of the mutagen ribavirin (RBV) resulted in a RBV-resistance mutation that conferred higher fidelity of the RdRp (G64S) (Pfeiffer and Kirkegaard, 2003). This specific mutation reduced the error frequency, thereby limiting reversion of additional

engineered mutations. Importantly, G64S poliovirus had reduced viral fitness during infection *in vivo*, indicating that diversity of a given viral population is necessary for virulence (Pfeiffer and Kirkegaard, 2005; Vignuzzi et al., 2005; Vignuzzi et al., 2006).

RNA viruses may overcome mutation-induced defects by several genetic mechanisms. First, error-prone RNA replication can revert mutations (Domingo and Holland, 1997; Drake, 1993). Second, genetic recombination can occur when two distinct viruses co-infect the same cell and exchange genetic information (Kirkegaard and Baltimore, 1986). Recombination can combine mutations on a single viral genome, or "erase" mutations by restoring the viral consensus sequence. Indeed, recombination of genomes has been observed with poliovirus and other enteroviruses (Arita et al., 2005; Cuervo et al., 2001; Dahourou et al., 2002; Furione et al., 1993; Holmblat et al., 2014; Sergiescu et al., 1969; Simmonds et al., 2005). Furthermore, defective genomes are capable of undergoing recombination and thus restoring their fitness *in vivo* (Holmblat et al., 2014). Individuals infected with VDPVs, particularly those that exhibit paralysis, are commonly infected with viruses that have undergone genetic exchange (Cherkasova et al., 2002; Dahourou et al., 2002; Furione et al., 1993; Liu et al., 2000). Third, fitness may be restored by complementation, whereby two viruses with distinct genetic defects co-infect a cell and these defects are complemented by the functional genome/protein. Complementation of poliovirus genomes has also been observed within brain tissues of infected mice (Vignuzzi et al., 2005). Fourth, fitness may be restored by reassortment. Reassortment can occur when two distinct, segmented viruses co-infect the same cell and generate progeny viruses containing a mixture of segments from both viruses. Genetic mechanisms such as recombination, complementation, and reassortment all

require a cell to be co-infected by two, or more, viruses. Overall, these events can promote viral diversity and may enhance pathogenesis of several RNA viruses (Dolan et al., 2018; Holmblat et al., 2014; Pfeiffer and Kirkegaard, 2005; Vignuzzi et al., 2006; Xiao et al., 2017).

Mechanisms of RNA virus co-infection

Several recent studies have shown that co-infection of RNA viruses can occur as a result of non-lytic, cell-to-cell transmission through membrane vesicle structures. During infection, poliovirus can be packaged in phosphatidylserine-rich vesicles (Chen et al., 2015). This mode of packaging facilitated the transport of several viral particles, and thus co-infection, to neighboring cells *in vitro* (Chen et al., 2015). More recently, it was demonstrated that norovirus and rotavirus can be shed in stool within vesicle structures derived from the host cell's endoplasmic reticulum or multi-vesicular body membranes, respectively (Santiana et al., 2018). Importantly, these vesicle-enclosed viruses were more infectious than single particles during fecal-oral transmission (Santiana et al., 2018). Additionally, poliovirus and CVB3 can exit cells through vesicles derived from autophagosomes, a process referred to as AWOL (autophagosome-mediated exit without lysis) (Bird et al., 2014; S. M. Robinson et al., 2014). Both hepatitis A and C viruses can exit infected cells through exosomes, or vesicle-like structures, thus mediating the transfer of infectious viral particles and RNA to neighboring cells *in vitro* (Dreux et al., 2012; Feng et al., 2013; Longatti et al., 2015; Ramakrishnaiah et al., 2013). These works highlight the existence of mechanisms that influence co-infection of RNA viruses, and potentially promote viral evolution.

Increasing evidence supports the idea that bacteria promote infection of mammalian viruses (Pfeiffer and Virgin, 2016). While it is clear that enteric viruses interact closely with the host microbiota, whether these bacteria influence diversity of these viruses had not been studied until recently. Our lab screened 40 bacterial strains for poliovirus binding and found that nearly all could bind the virus, and multiple virions could bind each bacterial cell (Erickson et al., 2018). Importantly, several of these bacterial strains induced the co-infection of distinct genetically marked polioviruses, even at a low MOI. Furthermore, co-infection of viruses correlated with the ability of bacteria to adhere to host cells. As a result of bacteria-mediated co-infection, genetic recombination occurred between two distinct parental strains with separate genetic defects, restoring viral fitness of progeny recombinant viruses. Additionally, our lab determined that bacteria can facilitate the co-infection of multiple distinct parental viruses, with up to 6 different parental viruses observed in a single plaque (Erickson et al., 2018). Overall, these findings indicate that bacteria mediate viral co-infection and may influence viral evolution.

THE MAMMALIAN INTESTINAL MICROBIOTA

The Mammalian Intestine

The mammalian intestine is a complex organ, home to various cell types and microorganisms, including commensal bacteria. The intestine is lined with intestinal epithelial cells (IECs) that benefit the host by absorbing nutrients and providing a physical barrier against the contents of the gut lumen, including the gut microbiota. Included in the

group of IECs are M cells, which can sample lumenal contents and transport them across the barrier. These contents can then be presented to dendritic cells and macrophages to induce necessary immune responses. In addition to the IEC barrier, the intestine is also lined with a dense inner mucus layer as an additional layer of protection, extending approximately 50 μM from IECs (Peterson and Artis, 2014; Vaishnava et al., 2011). This inner mucus layer is a 'bacteria free' zone. In the colon, an outer mucus layer is present, with both inner and out mucus layers extending approximately 150 μM from the IECs (Johansson et al., 2008; Peterson and Artis, 2014).

Apart from physical intestinal barriers, other secretory factors are present within the intestine and play an important role in homeostasis of the gut. Paneth cells secrete antimicrobial peptides (AMPs), such as defensins and lectins, that aid in defense against bacterial invasion (Peterson and Artis, 2014). Within this group of AMPs is regenerating islet-derived protein IIIγ (RegIIIγ), a C-type lectin that targets intestinal bacteria through recognition of the surface polysaccharide, peptidoglycan (PG) (further discussed in "bacterial surface molecules") (Cash et al., 2006). RegIIIγ was also shown to contribute to the spatial barrier of intestinal bacteria and the host (Vaishnava et al., 2011). AMPs are induced following recognition and activation of the intestinal immune response by pattern recognition receptors. An additional host factor that plays a role in intestinal homeostasis is secretory immunoglobulin A, the most abundant immunoglobulin within the host (Macpherson and Uhr, 2004; Suzuki et al., 2004). This secretory antibody limits bacterial invasion by binding directly to bacteria (Peterson and Artis, 2014). Additionally, this antibody controls poliovirus infection in infected individuals (Valtanen et al., 2000).

Ultimately, several host factors play important roles in maintaining symbiotic relationships within the intestine.

Enteric viruses, including poliovirus, encounter the complex environment of the intestine and face many barriers within the host. Following ingestion, these viruses encounter digestive enzymes within the saliva, stomach and small intestine of the host. Peristalsis, involuntary muscle contraction to induce movement of intestinal contents by the parasympathetic nervous system, moves the virus through differential pHs until it ultimately reaches its replication site in the lower part of the small intestine, the ileum (Huizinga and Lammers, 2009). The environment within the stomach is extremely acidic, maintaining pH values between 1.5 and 2 to aid in digestion. Poliovirus is acid tolerant, but there is some inactivation by the low gastric pH in PVRtg, IFNAR-/- mice (Ohka et al., 2007). Therefore, it is likely that low pH may also reduce the number of viable polioviruses able to reach the ileum. These factors, among others, contribute to the possibility that initial infection of enteric viruses is likely a low MOI event.

Host Intestine Bacterial Microbiota

The human gut microbiota is composed of bacteria, archaea, viruses, fungi and several other organisms (Pfeiffer and Virgin, 2016). An individual's microbiota begins establishing at the moment of birth. Each individual harbors a unique microbiota and the method of birth causes distinct differences in the initial microbiota that becomes established (Dominguez-Bello et al., 2010). Despite the unique differences in microbial composition of the gut between person to person, there are also distinct, commensal organisms that are shared amongst individuals. These organisms belong to four distinct

phyla of the bacterial kingdom, which includes Bacteroidetes, Firmicutes, Proteobacteria and Actinobacteria (Eckburg et al., 2005; Turnbaugh et al., 2009). The most abundant of these four phyla are the Bacteroides and Firmicutes (Eckburg et al., 2005; Turnbaugh et al., 2009). The phyla Bacteroides and Firmicutes, include Bacteroides and Clostridium, and Lactobacillus and Bacillus, respectively (Honda and Littman, 2012). Other factors that can also affect the composition of the microbial community include stress, changes in diet and administration/consumption of antibiotics. Overall, the hosts' intestinal microbiota play an important role in intestinal homeostasis, immunity and digestion (Honda and Littman, 2012).

Bacterial Surface Molecules

The intestinal microbiota is composed of over a trillion (10^{12}) bacteria from various phyla. These bacteria are designated as Gram-negative or Gram-positive according to the outcome of gram staining developed by Hans Gram in the late 1800s. Gram-negative bacteria appear pink after crystal violet staining due to their thinner layer of PG, whereas Gram-positive bacteria have a thick layer of PG that retain the violet dye after de-staining. Gram-negative bacteria have an outer membrane that contains lipopolysaccharide (LPS) on their surface. LPS is a disaccharide comprised of six to seven acyl chains, a polysaccharide core, and O-antigen (Silhavy et al., 2010). Gram-positive bacteria lack an outer membrane and are stained purple due to the retention of crystal violet within the thick layer of PG found on the outer surface. PG is composed of N-actelyglucosamine (GlcNac) and N-acetylmuramic acid chains (Silhavy et al., 2010). In addition to PG, Gram-positive bacteria also harbor lipoteichoic acids on the bacterial cell surface (Silhavy et al.,

2010). These surface compounds aid in bacterial identification as well as in bacterial cell shape, permeability and protection.

Mammalian virus-host microbiota interactions

In the last few years, studies from multiple groups have shown that intestinal bacteria play an important role in the infection of several unrelated RNA enteric viruses, including poliovirus, reovirus, rotavirus, mouse mammary tumor virus (MMTV) and noroviruses (Baldridge et al., 2015; Jones et al., 2014; Kane et al., 2011; S. K. Kuss et al., 2011; Uchiyama et al., 2014). Bacteria may promote viral infection through direct effects on viral particles or indirect effects on the host (Baldridge et al., 2015; Jones et al., 2014; Kane et al., 2011; S. K. Kuss et al., 2011; Li et al., 2015; Pfeiffer and Virgin, 2016; C. M. Robinson et al., 2014; Uchiyama et al., 2014). For poliovirus, the intestinal microbiota was required for efficient replication and pathogenesis in mice (S. K. Kuss et al., 2011). More specifically, bacteria increased the attachment of poliovirus to host cells in a poliovirus receptor (PVR)-dependent manner and also limited virion inactivation from heat or bleach treatment *in vitro* (S. K. Kuss et al., 2011; C. M. Robinson et al., 2014). The enhancement of poliovirus attachment requires polysaccharides that contain GlcNAc chains longer than 6 units (S. K. Kuss et al., 2011; C. M. Robinson et al., 2014). Our lab further determined that poliovirus binds to the surface of bacteria, indicating that direct interactions are mediating these observed effects (Erickson et al., 2018; S. K. Kuss et al., 2011; C. M. Robinson et al., 2014). Furthermore, this effect was observed using an unrelated enteric virus, reovirus, demonstrating that intestinal bacteria may have a similar effect on other enteric viruses (Berger et al., 2017; S. K. Kuss et al., 2011). Indirect

mechanisms of bacteria-mediated enhancement of enteric viral infection include modulation of the host immune response (Baldridge et al., 2015; Kane et al., 2011). During MMTV infection, interaction of MMTV with LPS activated TLR4 signaling and subsequent IL-10 production, leading to immune tolerance of the virus (Kane et al., 2011). Therefore, MMTV specifically required LPS to propagate within the mouse host (Kane et al., 2011). Intestinal bacteria that express certain histo-blood group antigens were required for infection of human norovirus *in vitro* and intestinal microbiota promoted murine norovirus replication *in vivo* (Jones et al., 2014). This finding ultimately led to the first cell culture system for human norovirus (Jones et al., 2014). For murine norovirus, bacteria may dampen IFN-λ mediated effects (Baldridge et al., 2015). Overall, it is clear that intestinal bacteria promote infection of mammalian viruses that replicate within the gut. Despite the recent advances in understanding the relationship between gut microbes and enteric viruses, understanding the effect that gut microbes have on other viruses related to poliovirus have yet to be fully defined. Overall, bacteria facilitate infection of several unrelated RNA viruses through several mechanisms.

CHAPTER TWO

Plaques Formed by Mutagenized Viral Populations Have Elevated Co-infection Frequencies

Introduction

Viral concentrations are frequently determined using the plaque assay, which is based on the principle that each plaque represents one infectious unit (Dulbecco and Vogt, 1953). Many mammalian viruses have high particle to plaque-forming unit (PFU) ratios due to various factors such as assembly defects, mutations, and inefficient steps during the viral replication cycle (Duarte et al., 1992; Muller, 1964; Yuste et al., 1999). For most mammalian viruses, the number of plaques is directly proportional to the concentration of virus. This indicates that one infectious particle gives rise to one plaque, providing a “one hit” model for plaque formation. However, certain viruses of plants and fungi have a “two hit” model, whereby two particles containing different genome segments are required to co-infect the same cell to facilitate productive infection and plaque formation (Ghabrial and Suzuki, 2009; Rao, 2006). Recently, Ladner *et al*. reported that a mammalian virus has a “three hit” model (Ladner et al., 2016). This virus is composed of five genome segments, each packaged in five separate viral particles; however, a minimum of three segments were required to facilitate productive infection. While previous work indicates that, for most mammalian viruses, plaque number appears to correlate linearly with the dilution of virus plated, it is possible that some plaques may be the products of co-infection.

Several mechanisms could facilitate co-infection of viruses. Previous reports demonstrated that cells may be infected by more than one virus at a higher frequency

than predicted by Poisson distribution (Bird and Kirkegaard, 2015; Bird et al., 2014; Chen et al., 2015; Combe et al., 2015; Shabram and Aguilar-Cordova, 2000). For example, poliovirus can be packaged in phosphatidylserine vesicles, which promotes co-infection of neighboring cells (Chen et al., 2015). Multiple coxsackievirus B3 and hepatitis A virions can also be packaged in vesicle-like structures (Feng et al., 2013; S. M. Robinson et al., 2014). Vesicular stomatitis virus was found to form plaques containing two different viral genomes, indicating that co-infection occurred (Combe et al., 2015). Additionally, many different viruses aggregate in solution and could induce co-infection (Floyd and Sharp, 1977, 1978, 1979; Wallis and Melnick, 1967). Viral stocks of vaccinia virus, influenza virus, adenovirus, herpes virus, and echovirus contained virion aggregates that were resistant to antibody-mediated neutralization and/or radiation (Sharp and Dunlap, 1966; Wallis and Melnick, 1967). Poliovirus and reovirus particles can aggregate in sewage, which may contribute to initial infection of the host and it is possible that virion aggregates exist *in vivo* (Sharp et al., 1975; Young and Sharp, 1977).

RNA viruses undergo error-prone replication due to lack of proofreading activity of their RNA-dependent RNA polymerase (RdRp). Much has been learned about RNA virus mutation-associated fitness effects from viral populations harboring increased or decreased mutation frequencies. Crotty *et al*. demonstrated that the nucleoside analog RBV is an RNA virus mutagen. RBV is incorporated into nascent RNA by the viral RdRp, which increases transition mutations and can cause “error catastrophe” (Crotty et al., 2001). Conversely, poliovirus passaged in the presence of RBV acquired a single point mutation in the RdRp, G64S, which increased fidelity of viral RNA synthesis and reduced the error frequency of the viral population (Arnold et al., 2005; Pfeiffer and Kirkegaard,

2003)**.** Importantly, G64S poliovirus had reduced viral fitness during infection of mice, indicating that viral population diversity is necessary for virulence (Pfeiffer and Kirkegaard, 2005; Vignuzzi et al., 2005).

RNA viruses may overcome mutation-induced fitness costs by several genetic mechanisms (Domingo and Holland, 1997). These include reversion, recombination, reassortment and complementation (discussed in “mechanisms of RNA virus co-infection”). Overall, these genetic processes can alter viral diversity and increase fitness.

In this work, I examined whether viral plaques are derived from a single founder and whether viruses with increased genome damage may be more reliant on co-infection for plaque formation. Through the use of a genetic assay with ten distinct polioviruses and a phenotypic assay with two distinct polioviruses, I have shown that multiple parental viruses can be found within a single plaque, which I refer to as a chimeric plaque. I determined that 5-7% of plaques were derived from two or more viruses. To assess factors contributing to co-infection, I used dynamic light scattering and electron microscopy to demonstrate that viral stocks contain both single particles and aggregates, suggesting that infection with virion aggregates is likely responsible for chimeric plaque formation. Indeed, inducing virion aggregation via exposure to low pH increased co-infection frequency in a separate flow cytometry-based assay. I examined whether there were situations where co-infection frequencies varied and whether co-infection may assist plaque formation. Using high fidelity G64S polioviruses that harbor fewer mutations than wild-type (WT) and RBV-mutagenized polioviruses that harbor more mutations than WT, I found that co-infection frequency correlated with mutation load. In fact, 17% of plaques from mutagenized virus infections were the product of co-infection. This work indicates

more than one virus can contribute to plaque formation and that co-infection may assist plaque formation in situations where the amount of genome damage is high.

Materials and Methods

*Cells and viruses***.**

HeLa cells were propagated in Dulbecco's modified Eagle's medium (DMEM) supplemented with 10% calf serum and 1% penicillin/streptomycin. All infections were performed using viruses derived from Mahoney serotype 1 infectious cDNA clone variants containing WT-RdRp, G64S-RdRp, with or without *3NC-202gua*^{R} mutations (see Fig. 5A for schematic) (Kirkegaard and Baltimore, 1986; Pfeiffer and Kirkegaard, 2003). The *3NC-202gua*^{R} virus contains two mutations that confer guanidine resistance (2C-M187L and 2C-V250A) and an insertion in the 3' non-coding region that confers temperature sensitivity (3-NC202) (Kirkegaard and Baltimore, 1986; Sarnow et al., 1986). To generate highly-mutagenized poliovirus, 1 x 10^6 HeLa cells were pre-treated with 800 μM RBV (Sigma) for 1 h. Approximately 1 x 10^5 plaque-forming units (PFU) of virus was used to infect the cells for 30 min at 37°C and 5% CO_2. Unattached virus was washed with PBS and media containing 800 μM RBV was added to the cells. Virus was harvested at approximately 7 hours post infection (hpi) in 1 mL phosphate-buffered saline supplemented with 100 μg/mL $CaCl_2$ and 100 μg/mL $MgCl_2$ (PBS+). Passage of virus in the presence of RBV was repeated 4-5 times. For the genotypic assay, ten polioviruses derived from Mahoney serotype 1, each containing unique silent point mutations in the VP3-capsid coding region, were used as previously described (Kuss et al., 2008).

Quantifying dual parent vs. single parent plaque viruses.

The ten polioviruses containing unique silent point mutations were mixed in equivalent amounts with PBS+ and incubated at 37°C for 1 h. After incubation, the viral mixture was diluted to a multiplicity of infection (MOI) of ~0.00001 and plated onto 10 cm plates seeded with 1 x 10^6 HeLa cells. After attachment, unbound virus was removed and an agar overlay was added as previously described (Pfeiffer and Kirkegaard, 2003). Plates were incubated at 37°C and 5% CO_2 for 48 h, plaques were picked, and plaque agar plugs were placed into tubes containing 1 ml PBS+. Plaque stocks were freeze-thawed three times to release virus and 200 µl of these viruses were used to infect fresh HeLa cells to generate viral RNA for analysis of parental viruses. At 6 hpi, total RNA was isolated using TRI-Reagent (Sigma-Aldrich) according to the manufacturer's instructions. cDNA synthesis, PCR, blotting, and hybridization using ^{32}P-labeled oligonucleotide probes specific for each of the ten viral sequences was performed as previously described (Kuss et al., 2008).

In the phenotypic assay, 1 x 10^5 PFU of $Drug^S/Temp^R$ poliovirus and $Drug^R/Temp^S$ poliovirus were incubated in PBS+ for 1 h at 37°C. After incubation, the viral mixture was diluted to a MOI of ~0.00001 and plated onto 10 cm plates seeded with 1 x 10^6 HeLa cells. After attachment, unbound virus was removed and agar overlay was added as previously described (Pfeiffer and Kirkegaard, 2003). Plates were incubated at 33°C and 5% CO_2 in the absence of guanidine hydrochloride (Sigma) for 4-5 days. Plaques were picked and placed into tubes containing 1 mL PBS+. To release virus, plaques stocks were freeze-thawed three times prior to screening. Plaque viruses were screened by performing plaque assays under selective growth conditions (33°C with 1 mM guanidine

or 39°C without guanidine). To ensure that phenotypes could be discriminated accurately, trial blinded experiments were performed and $Drug^S/Temp^R$ vs. $Drug^R/Temp^S$ viruses were correctly scored. Of several hundred plaques that were picked during the course of this study, 14 did not contain detectable virus and were not included in the analysis. It is likely that these "plaques" were non-viral defects in the monolayer. Because no detectable virus was present in these samples, it is unlikely that inefficient/abortive infections that yield low-level virus are common in this system.

Analysis of poliovirus aggregation by electron microscopy.

Poliovirus stocks were purified by cesium chloride gradient centrifugation and were concentrated and desalted using Amicon filters (Millipore) as previously described (S.K. Kuss et al., 2011). Poliovirus samples containing 9.3 x 10^6 PFU were inactivated by treating with 2.5% glutaraldehyde for 1 h at room temperature. After inactivation, 2.5 µl of the inactivated virus was placed on 400 mesh carbon-coated copper grids that had been glow discharged for 30 s using PELCO EasiGlow™ 91000. Grids were stained with 2% phosphotungstic acid and examined using a TEI Technai G^2 Spirit Biotwin transmission electron microscope (FEI, Hillsboro, OR) equipped with a Gatan ultrascan CCD camera, operated at an acceleration voltage of 120 kV. Images were taken at a magnification of 13,000x and 30,000x.

Quantifying poliovirus aggregation using dynamic light scattering.

Samples of 5 x 10^4 PFU gradient purified poliovirus (see electron microscopy methods above) were prepared in a total volume of 20 µL and samples were centrifuged

at 10,000 rpm for 10 min before data acquisition to remove dust or contaminants. Experiments were performed on a Protein Solutions DynaPro instrument equipped with a temperature-controlled microsampler (Wyatt Technology) using 20 s acquisition time and 20% laser power. Each measurement was an average of 20 data points. The data were processed with the program Dynamics V6. The radii and the size distribution were calculated with the regularization algorithm provided by the software.

Flow cytometry-based assay for co-infection.

Viruses derived from Mahoney serotype 1 infectious cDNA clone (PV) encoding *Aequorea coerulescens* GFP (GFP) or *Discosoma sp.* red (DsRed) fluorescent proteins inserted after amino acid 144 of PV protein 2A (PV-2A144-GFP and PV-2A144-DsRed) have been previously described (Teterina et al., 2010). Equal amounts of GFP-PV and DsRed-PV (1×10^4 PFU each) were incubated in 200 µL of PBS (pH 7.4) or 0.05 M glycine-hydrochloride (glycine-HCL)/H_2O buffer (pH 3) for 4 h at room temperature. HeLa cells grown in 6-well plates containing approximately 2×10^6 cells/well were mock infected with pH 3 buffer or infected with the GFP- and/or DsRed-PV mixtures for 15 min at 37°C. The cells were washed with PBS and 2 mL of DMEM supplemented with 5% calf serum and 1% penicillin/streptomycin was added to each well. After incubation for 16 h at 37°C and 5% CO_2, cells were harvested using 0.1% trypsin/0.05% EDTA solution, washed and fixed with 2% paraformaldehyde fixation solution for 15 min at room temperature and resuspended in 300 µL 2% fetal bovine serum/PBS. Expression of GFP and DsRed was determined using a FACSCalibur cytometer equipped with 488- and 635-nm lasers. FACS data were analyzed using FlowJo software. Given the low MOI, a relatively large

number of cells (2 x 10^5) were counted for each experimental condition. Experiments performed with a range of MOIs demonstrated that the conditions used here were in the linear range and above the detection limit (data not shown). Additionally, the observed co-infection frequency of 0.0048% is nearly identical to the co-infection frequency predicted by Poisson's distribution (0.005%) (Fig. 4E). Gates were determined using uninfected cells or singly infected cells as indicated in the legend for Figure 4.

Quantifying mutation frequency of viruses.

Error frequencies were determined by acquisition of guanidine resistance, as previously described (Pfeiffer and Kirkegaard, 2003). Because the $Drug^R/Temp^S$ viruses are uninformative for this assay, I scored the frequency of guanidine resistance in the $Drug^S/Temp^R$ viruses (grown in parallel with the $Drug^R/Temp^S$ viruses) in the 1) WT-RdRp background, 2) G64S-RdRp background, or 3) WT-RdRp background mutagenized with RBV (see Fig. 4A for schematic). Viral dilutions were plated on approximately 1 x 10^6 HeLa cells to determine viral titer by plaque assay at 33°C and 39°C in the presence or absence of 1 mM guanidine hydrochloride. The error frequencies were determined by dividing PFU/mL obtained in the presence of drug by PFU/mL in the absence of drug. Note that the highest observed error frequency ($Drug^R$ reversion frequency) was 1.6 x 10^3, meaning that 1 in every 625 viruses lost the guanidine resistance phenotype. Because the number of plaques screened in the phenotypic assay is much lower than this reversion frequency, it is unlikely that gain or loss of the $Drug^R$ marker impacted quantification of co-infection. To quantify the relative specific infectivity for WT-RdRp, G64S-RdRp, and WT-RdRp + RBV stocks, RNA was extracted from 1 x 10^6 PFU of each

stock using TRI-Reagent (Sigma) with carrier RNA from 10^6 HeLa cells, and quantification of poliovirus RNA was performed using quantitative RT-PCR. Reverse transcription was performed with Superscript II (Invitrogen) using an antisense primer 5′ TGTAACGCCTC CAAATTC CAC 3′ in the VP2-capsid coding region. To perform qPCR, 5 µL of the cDNA reaction was mixed with SYBR green PCR master mix reagent (Applied Biosystems) and 10 µM of each primer. The VP2 capsid region was amplified with the sense primer 5' TGAGGGA CATGGGACTCTTT 3' and the antisense primer above using an Applied Biosystems 7500 system. Cycling conditions were: 1 cycle for 2 min at 50°C and 10 min at 95°C, followed by 40 cycles of 15 sec at 95°C and 1 min at 60°C. The qPCR reactions were performed in duplicate from two independent RNA preparations and quantified using standard curve generated with poliovirus plasmid DNA samples. Analysis of standard curve and data were determined as previously described (Bookout et al., 2006; Ibarra and Pfeiffer, 2009). Specific infectivity was determined by dividing 1 x 10^6 PFU by the relative RNA amounts (Table 2).

Relationship between virus dilution and plaque numbers at different co-infection frequencies.

To generate the graph shown in Figure 6, I used the following formula to calculate the predicted number of plaques generated by several dilutions of virus over a range of co-infection frequencies: [(Dilution)^1 x Fraction with 1 Virus] + [(Dilution)^2 x Fraction with 2 Viruses]= # Plaques.

Results

A small percentage of plaques are derived from more than one parental virus.

To determine whether plaques are the product of more than one founding virus, distinct parental viruses that can be discriminated by genotype or phenotype are required. I began by using ten genetically distinct polioviruses that each contain unique silent point mutations and are discriminated by hybridization of RT-PCR products with specific probes. I previously demonstrated that these ten marked viruses are equally fit (Kuss et al., 2008; Lancaster and Pfeiffer, 2010; Luethy et al., 2016). I mixed equal amounts of the ten viruses and infected HeLa cells at an extremely low MOI such that ~2-20 plaques would be generated on each plate of 10^6 cells (Fig. 1A). Plaques were picked, viruses were amplified for a single cycle in HeLa cells, and the presence of each virus was determined by probe-specific hybridization of RT-PCR products (Kuss et al., 2008; Lancaster and Pfeiffer, 2010; Luethy et al., 2016). Plaques were scored as having a single parent virus (e.g. Plaque 1) or more than one parent virus (e.g. Plaque 2) (Fig. 1B). I examined whether each of the ten viruses were equally represented in plaques since skewed ratios of the input viruses could impact the observed frequency of co-infection. The distribution of viruses present within all plaques tested was reasonably even, with each of the ten viruses nearly equally represented (Fig. 1C). Of 123 total plaques analyzed, 6 had more than one founding parental viruses and 117 had a single virus (Table 1). Therefore, 4.9% of plaques were derived from more than one parental virus.

It was possible that overlapping plaques with single parental viruses were picked and incorrectly scored as chimeric. If so, the frequency of chimeric plaques should be higher on plates with more plaques present. To rule out the possibility that picking dual-

parent plaques was enriched in situations where a higher number of plaques were present on the plate, I compared the number of plaques on plates from single and dual parent plaques (Fig. 1D). I found that dual parent plaques were not more prevalent on plates with higher plaque numbers, indicating that cross-contamination of plaque viruses was unlikely.

Since the ten virus genotypic assay to measure co-infection is relatively labor intensive, I sought to simplify the screening process by using a previously characterized poliovirus mutant that can be discriminated from WT by a phenotypic assay (Kirkegaard and Baltimore, 1986) (Fig. 2A). *3NC-202gua*^{R} poliovirus has mutations that confer resistance to guanidine hydrochloride and temperature sensitivity (called Drug^{R}/Temp^{S} hereafter). Guanidine is used as a protein denaturant but can also specifically inhibit poliovirus RNA synthesis (Tershak, 1982)**.** Conversely, WT poliovirus is guanidine sensitive and temperature resistant (called Drug^{S}/Temp^{R} hereafter). I mixed equal amounts of Drug^{R}/Temp^{S} and Drug^{S}/Temp^{R} polioviruses and infected HeLa cells at an extremely low MOI such that ~2-20 plaques would be generated on each plate of 10^{6} cells. Infections were incubated in permissive conditions for both parental viruses (33°C without drug). Plaques were picked and analyzed by their growth phenotypes to determine whether one or both parental viruses were present. Plaque formation at 33°C in the presence of drug indicated the presence of the Drug^{R}/Temp^{S} parent. Plaque formation at 39°C indicated the presence of the Drug^{S}/Temp^{R} parent. Plaque formation in both conditions indicated presence of both parental viruses (Fig. 2C). The distribution of viruses present within plaques was reasonably even, with 44.2% and 55.8% of Drug^{S}/Temp^{R} and Drug^{R}/Temp^{S} parental viruses, respectively (Fig. 2C). In this assay, I

found that 10 out of 138 (7.3%) plaques had more than one parental virus present (Table 1). Therefore, both the genotypic and phenotypic assays indicate that ~5-7% of plaques that arise following infection of HeLa cells contain more than one distinct parental virus.

Poliovirus stocks contain viral aggregates.

To examine whether co-infection of poliovirus may be due to viral aggregation, I examined representative viral stocks using visual and biophysical assays. I first examined viruses using electron microscopy and observed single viral particles as well as aggregated viral particles (Fig. 3A), in agreement with previous studies (Floyd and Sharp, 1977, 1978, 1979)**.** To quantify poliovirus aggregation, I used dynamic light scattering, which measures the size of particles in solution. Using this assay, I observed that my viral stock contained both single particles (15 nm radius) and aggregates ranging from 2-10 particles (Fig. 3B). Overall, these results indicate that viral stocks contain aggregates and I speculated that virion aggregation facilitates co-infection of viruses*.*

*Inducing aggregation increases co-infection frequency***.**

To test the hypothesis that virion aggregation facilitates co-infection, I examined co-infection frequency for virions exposed to conditions that induce aggregation using a minimally labor-intensive flow cytometry-based assay. Polioviruses expressing either GFP or DsRed (Teterina et al., 2010) were mixed and incubated for 4 h in PBS (control) or in glycine-HCL buffer, pH 3, which induces aggregation of poliovirus (Floyd and Sharp, 1977, 1978, 1979) (Fig. 4A). Viruses were then used to infect HeLa cells at an MOI of 0.01, such that ~99% of cells remain uninfected. Sixteen hours post-infection, cells were

subjected to flow cytometry to quantify the percentage of uninfected, singly infected (red or green), or co-infected cells (red and green, dual positive). To ensure that the low pH treatment induced virion aggregation, I measured particle size using dynamic light scattering. Indeed, viruses exposed to low pH had increased radii compared with viruses exposed to PBS, confirming that low pH induced virion aggregation (Fig. 4B). Based upon an MOI of 0.01, approximately 1% of cells infected with PBS-treated viruses were infected with a single virus (Fig. 4C). However, 0.83% of cells infected with low pH-treated viruses were infected with a single virus, suggesting that virion aggregation slightly reduced the total number of infectious units. A small percentage, 0.0048%, of cells infected with PBS-treated viruses were co-infected with both DsRed- and GFP-expressing viruses (Fig. 4D), which is close to the predicted number of co-infected cells based on Poisson distribution (0.005%). Interestingly, co-infection was increased 2.6-fold in low pH-treated viruses, suggesting that aggregation enhances co-infection. Furthermore, these data indicate that co-infection can occur during infections performed in liquid culture.

Co-infection frequency correlates with mutation frequency.

I hypothesized that co-infection would rescue plaque formation for heavily mutagenized viruses due to processes such as complementation and recombination. Conversely, I hypothesized that viruses with fewer mutations would be less reliant on co-infection for plaque formation. To test this, I compared chimeric plaque frequencies of virus stocks with low, intermediate, or high mutation frequencies (Fig. 5). I used the existing data for the $Drug^S/Temp^R$ and $Drug^R/Temp^S$ viruses containing WT RdRp as a proxy for intermediate error frequency populations. To test viruses with low error

frequencies, I used Drug^S/Temp^R and Drug^R/Temp^S viruses harboring the G64S mutation in the RdRp, which confers higher fidelity. G64S-RdRp viruses and WT-RdRp viruses were equally fit in cell culture and grew to similar titers, but G64S-RdRp viruses had 4.5-fold fewer mutations than WT-RdRp viruses, in agreement with previous studies (Table 2) (Arnold et al., 2005; Pfeiffer and Kirkegaard, 2003). To test viruses with high error frequencies, I used Drug^S/Temp^R and Drug^R/Temp^S viruses passaged in the presence of RBV. For each virus, I infected HeLa cells in the presence of 800 μM RBV for a single cycle of replication, harvested progeny viruses and repeated this cycle 4-5 times to generate mutagenized viral populations. In agreement with previous studies, these mutagenized viruses had reduced fitness, with 8.3-fold lower titers and 21-fold more mutations than viruses passaged in the absence of RBV (Table 2)(Crotty et al., 2001). To confirm that mutagenized viral genomes had reduced specific infectivity compared with non-mutagenized WT-RdRp or G64S-RdRp viral genomes, viral RNA was extracted from 1 x 10^6 PFU and quantified by qRT-PCR. Indeed, RBV-mutagenized viruses required 2.5-fold or 3.4-fold more RNA to form the same number of plaques as WT-RdRP or G64S-RdRp viruses, respectively (Table 2). Therefore, these mutagenized viruses formed fewer plaques than non-mutagenized viruses due to reduced specific infectivity of their RNA genomes (Table 2) (Crotty et al., 2001). I performed mixed infections for each matched set of Drug^S/Temp^R and Drug^R/Temp^S viruses [high fidelity (G64S-RdRp) or low fidelity (WT-RdRp + RBV)] and determined the co-infection frequency using the phenotypic assay (Fig. 2, Fig. 5A). I observed that the co-infection frequency with G64S-RdRp viruses was decreased (3.2%) in comparison to the WT-RdRp viruses (7.3%) (Fig. 5B, Table 2). Additionally, viruses passaged in the presence of RBV had the highest

percentage (16.7%) of co-infection (Fig. 5B). Overall, these data show that co-infection frequency correlates with the error frequency of the viral population, with increased co-infection among plaques generated by heavily mutagenized viruses.

Discussion

Co-infection of RNA viruses can promote genetic diversity and emergence of novel viruses. I found that some plaques are the result of co-infection and contain two or more parental viruses. Furthermore, I determined that co-infection frequency correlates with the level of mutation-induced genome damage. Importantly, these effects would have been masked had I not used genetically distinct viruses.

My data show that 3-17% of plaques contain more than one founding virus. These data fall out of line with the 'one hit' model for plaque formation whereby one infectious particle gives rise to one plaque (Fig. 6, calculation depicted by dotted black line). Certain viruses of plant and fungi have a two hit model, whereby two particles containing different genome segments are required to co-infect the same cell to facilitate productive infection (Fig. 6, calculated depicted by dotted red line) (Ghabrial and Suzuki, 2009; Rao, 2006). I used the observed percentages of chimeric plaques to calculate the theoretical relationship between virus dilution and number of plaques. As shown in Figure 6, these lines all fall between the one hit and two hit model lines, although all are much closer to the one hit model line. Nonetheless, even this relatively low level of co-infection confers a slight "bend" to the one-hit model line, particularly for RBV-mutagenized viruses. These results indicate that the relationship between viral dilution plated and number of plaques is not linear, particularly for mutagenized viruses. Furthermore, even at extremely low

MOIs, cells may be infected with more than one virus at a higher frequency than predicted by Poisson distribution.

Although the data presented here indicate that 3-17% of plaques arose from co-infection of two different parental viruses, the actual frequency is likely higher because only one-third of possible co-infection events are observable in the phenotypic assay. For example, co-infection with the same parental virus (e.g., $Drug^{S}/Temp^{R}$ + $Drug^{S}/Temp^{R}$ or $Drug^{R}/Temp^{S}$ + $Drug^{R}/Temp^{S}$) is scored as single parent plaques in the phenotypic assay. Additionally, the presence of three or more parental viruses cannot be scored by the phenotypic assay. Indeed, using the genotypic assay, one plaque contained three of the ten parental viruses (data not shown). Furthermore, pre-aggregated viruses within parental virus stocks may limit even “mixing” and re-aggregation with viruses from other parental virus stocks, which could limit observable co-infection in this system. Therefore, the observed chimeric plaque frequencies (3-17%) are likely underestimates and the actual frequency of plaques containing more than one parental virus could be up to three times higher. For non-mutagenized viral populations, these frequencies of chimeric plaques would still fall relatively close to the linear one-hit model line (e.g., the green line in Fig. 6), making standard plaque assay dilution series appear nearly linear and/or within standard deviation of the assay. However, for mutagenized viral populations, the relationship between dilution plated and plaque number could become non-linear enough to affect quantification of virus concentration. If the observed chimeric plaque frequency is underestimated by three-fold for mutagenized viruses, 50% of plaques would be the product of co-infection and the relationship between dilution plated and plaque number becomes obviously non-linear (see orange line in Fig. 6). Although the observed co-

infection frequencies may be underestimates, several factors may limit productive co-infection. For example, some virions in a population are non-viable because they lack a genome and therefore cannot productively infect or co-infect a cell. Additionally, virion aggregates in my stocks were generally composed of a small number of virions. These types of factors pose an upper limit on co-infection frequency and chimeric plaque formation.

My work demonstrates that plaque formation correlates with the amount of genome damage present within the viral genome, perhaps due to restoration of fitness via recombination or complementation. Given that RNA viruses have high particle to PFU ratios, partly because of mutations, it is possible that co-infection-mediated fitness restoration could promote ‘viral resurrection’ of defective genomes. Overall, my findings indicate that multiple virions can contribute to plaque formation.

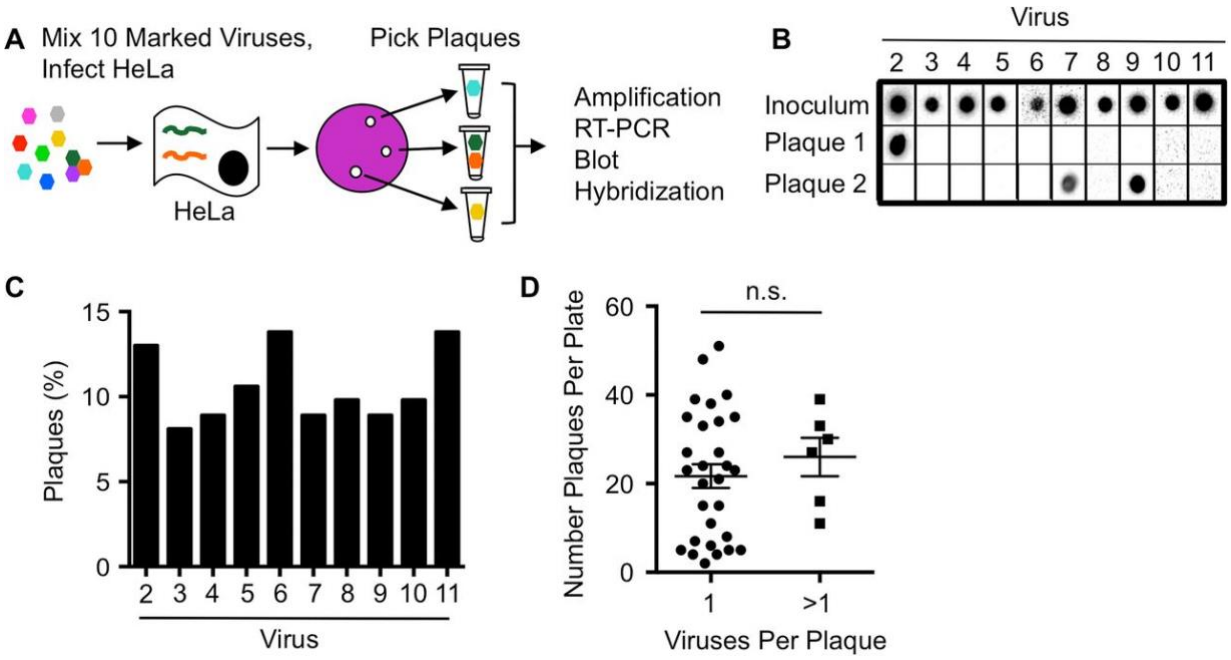

Figure 1. Genotypic assay reveals co-infection of polioviruses. (A) Schematic of assay design. HeLa cells were infected at an MOI of ~0.00001 with an equal mixture of ten genetically marked viruses. Hypothetical genomes are depicted in a HeLa cell. Plaques were picked from the agar overlays after incubation at 37°C for 48 h. Plaque viruses were amplified by infecting new cells and RT-PCR products were blotted and probed on a membrane to identify the virus(es) present. (B) Representative plaque virus samples detected by probes. The number of viruses present within each plaque was quantified. (C) Distribution of the ten marked viruses among all plaques. (D) Frequency of co-infected or non co-infected plaque viruses versus the number of plaques per plate, with mean ± standard error of the mean (difference not significant [n.s.], determined by Student's *t*-test).

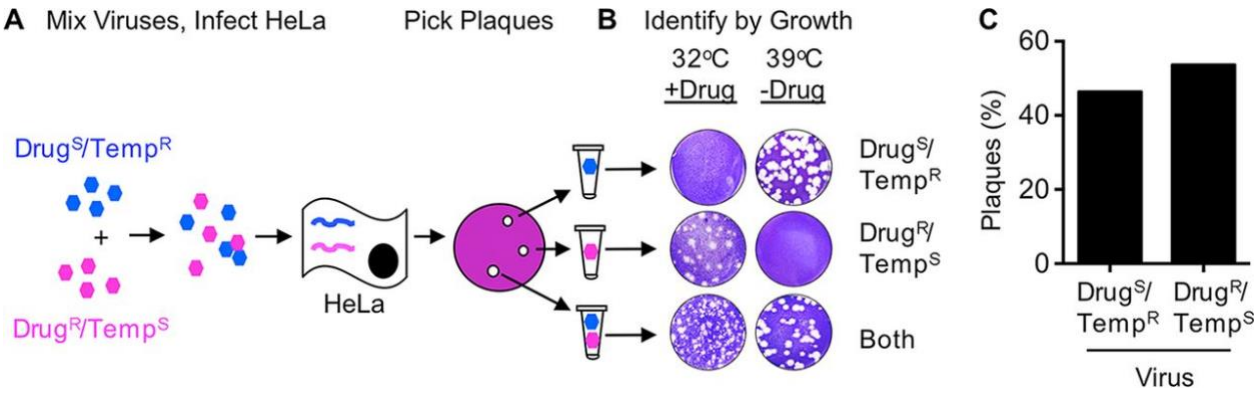

Figure 2. Phenotypic assay reveals co-infection of polioviruses. (A) Schematic of co-infection assay using Drug^{S}/Temp^{R} and Drug^{R}/Temp^{S} viruses. The two parental viruses were mixed, incubated and HeLa cells were infected with the viral mixture at an MOI of ~0.00001. Hypothetical viral genomes are depicted in a HeLa cell. Plaques were picked 4-5 days after adding agar overlay at 33°C in the absence of guanidine (permissive conditions). (B) Representative plaques in the phenotypic scoring assay. Plaque viruses were plated on HeLa cells under dual selective conditions as indicated. (C) Distribution of the two parental viruses among all plaques.

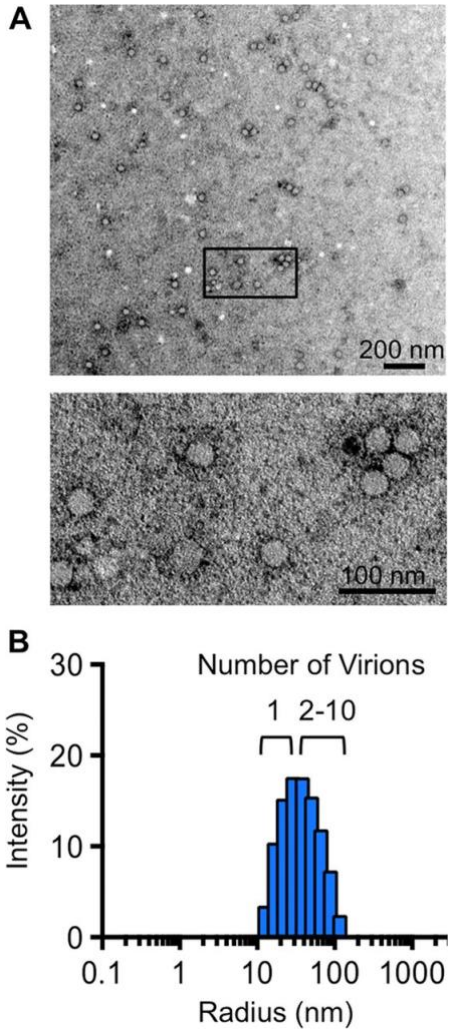

Figure 3. Stocks of poliovirus contain aggregates. (A) Transmission electron microscopy of a representative poliovirus stock. Viral particles were imaged at a magnification of 13,000x (top image) or 30,000x (bottom image, a detail of the boxed region in the top image). (B) Dynamic light scattering analysis of a representative poliovirus stock. Virus stock was diluted to 5 x 10^4 PFU/mL and centrifuged for 10 min prior to analysis on a Protein Solutions DynaPro instrument. Poliovirus radius = 15 nm.

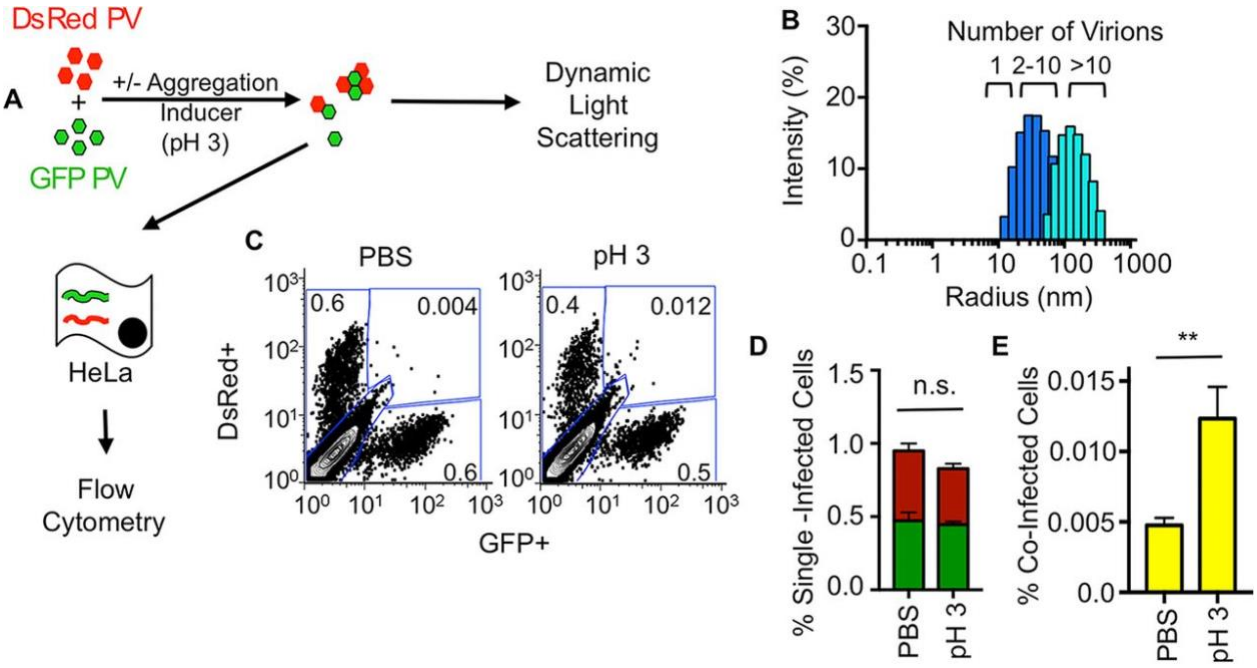

Figure 4. Flow cytometry-based assay demonstrates correlation between aggregation and co-infection. (A) Schematic of flow cytometry-based assay. GFP- and DsRed-expressing polioviruses were mixed in the presence or absence of aggregation inducing conditions (+/- exposure to pH 3 solution for 4 h) prior to analysis by dynamic light scattering or infection of HeLa cells at an MOI of 0.01. At 16 hpi, infection was quantified using flow cytometry. (B) Dynamic light scattering analysis of viruses exposed to PBS (royal blue, same data as in Fig. 3B) or viruses exposed to pH 3 glycine-HCL buffer for 4 h (turquoise). Samples were processed as described in Fig. 3. (C) Representative FACS plots showing quantification of DsRed, GFP, or dual positive cells. The units for x- and y-axes are GFP and DsRed fluorescence intensity, respectively. The numbers in each gate indicate the percentage positive of the total cell population of 2 x 10^5 cells counted. Gates were drawn from FACS plots of HeLa cells exposed to pH 3 glycine-HCL in the absence of PV (lower left gate), infected with 1 x 10^4 PFU GFP-PV (lower right gate), infected with 1 x 10^4 PFU DsRed-PV (upper left gate) or infected with 1 x 10^4 PFU GFP-PV and 1 x 10^4 PFU DsRed-PV (upper right gate) (D) Percentage of cells infected by single viruses (GFP or DsRed). (E) Percentage of co-infected cells, positive for both GFP and DsRed (upper right gate). Results are presented as mean ± standard error of the mean (n=9). Statistical significance was determined by Student's *t*-test, ***P*<0.005; n.s., not significant.

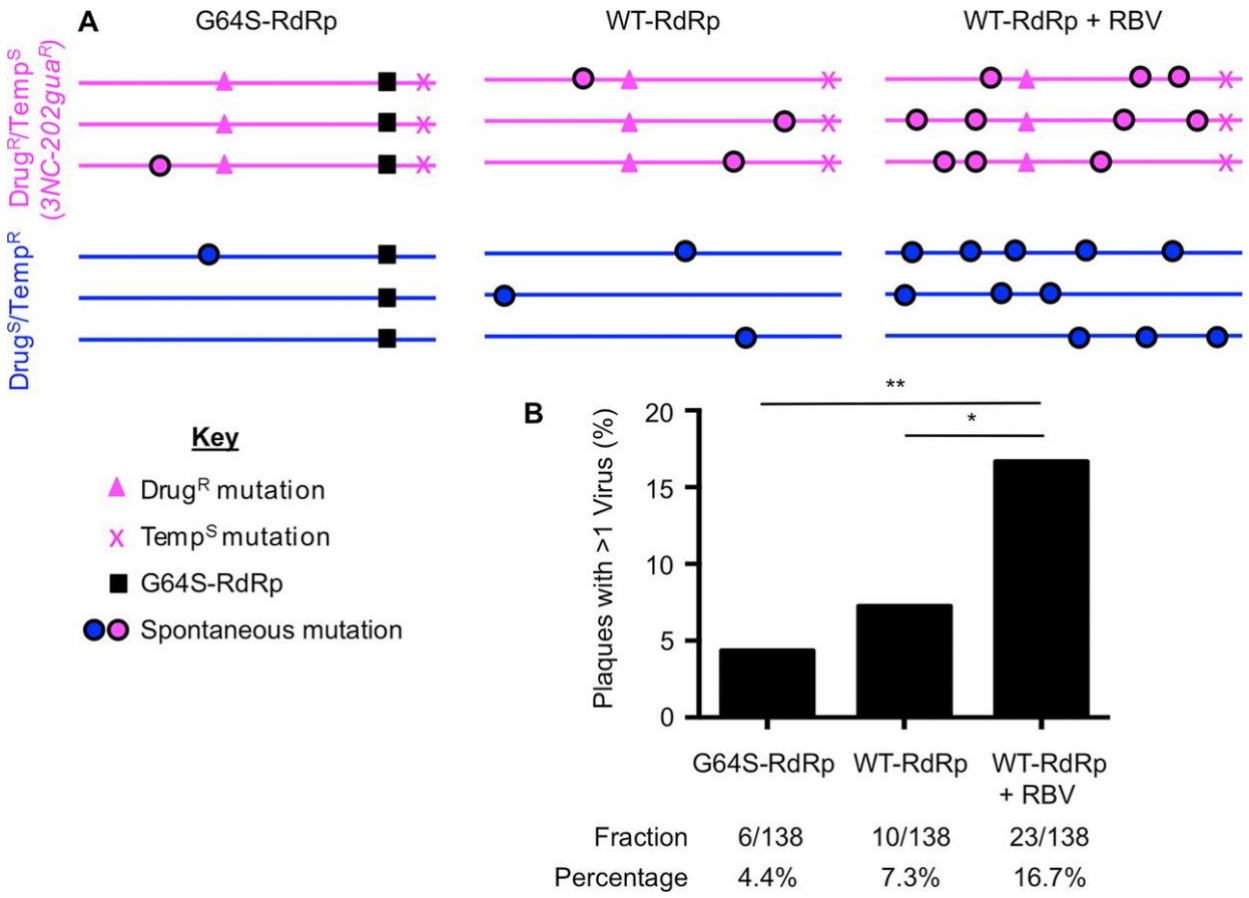

Figure 5. Co-infection frequency of poliovirus correlates with genome damage. (A) Schematic of viral genomes showing engineered vs. representative spontaneous mutations. (B) Co-infection frequencies of high fidelity/low mutation viruses (G64S-RdRp), intermediate mutation viruses (WT-RdRp) and high mutation viruses (WT-RdRp viruses + RBV) were performed as described for the phenotypic assay (Fig. 2). The value of co-infection for WT-RdRp is the same as presented in Table 1 for the phenotypic assay. Statistically significant differences were observed between WT-RdRp and WT-RdRp+RBV (**P*=0.0248), and between G64S-RdRp and WT-RdRp+RBV (***P*=0.0013) using Fisher's Exact Test.

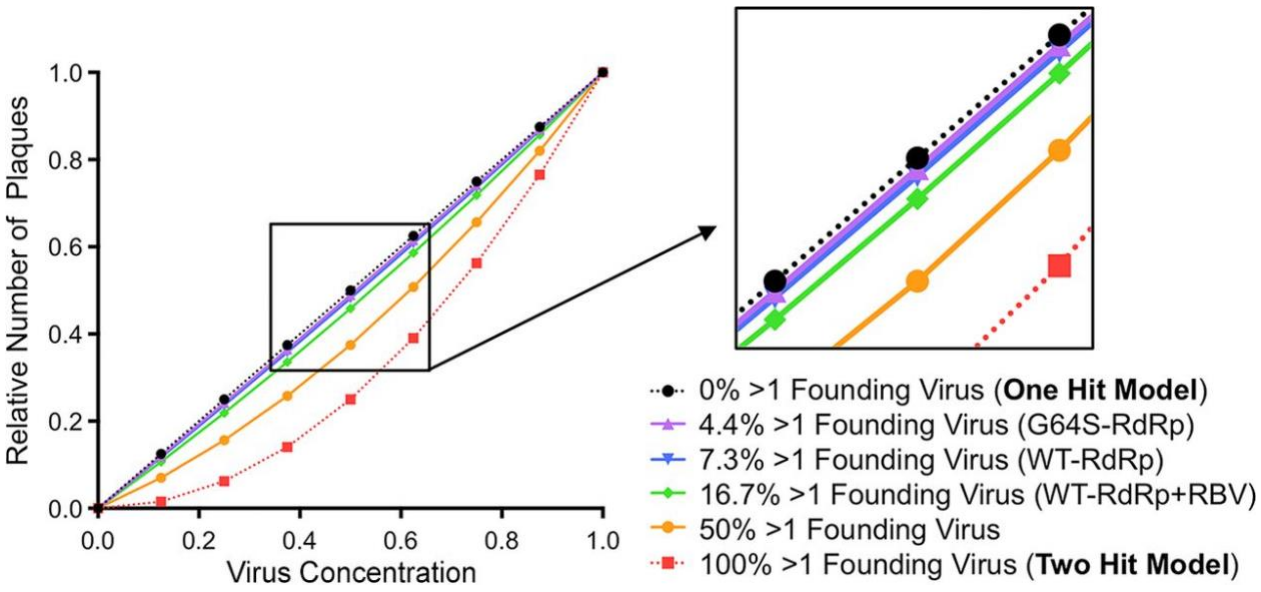

Figure 6. Theoretical relationship between virus dilution and plaque numbers at different co-infection frequencies. Plaque assays are based on the dose-response curve of a one-hit model (calculation depicted by dotted black line) where each plaque is formed by one infectious unit. Certain plant and fungal viruses have two-hit kinetics (calculation depicted by dotted red line), where two viral genomes per cell are required for productive infection and plaque formation. Purple, blue and green lines represent calculations using data obtained in Figure 5 for G64S-RdRp, WT-RdRp, and WT-RdRp + RBV viruses, respectively. Solid orange line represents theoretical curve for co-infection frequency of 50%. At low co-infection frequencies (e.g. 3.2% and 7.3%) the curvature of the lines are minimal and therefore the relationship between dilution and the number of plaques is nearly linear (see inset).

Table 1. Frequency of plaques with more than one founding/parental virus.

System	Fraction with > 1 virus	Percent with > 1 virus
10 Virus Genotypic Assay[a]	6/123	4.9%
2 Virus Phenotypic Assay[b]	10/138	7.3%

[a] Assay described in Figure 1
[b] Assay described in Figure 2

Table 2. Generating virus populations with different error frequencies.

Virus	Titer[a]	Error frequency[c]	RNA copies per 1 x 10^6 PFU[d]	Specific infectivity[e]
G64S-RdRp	2.9 x 10^9 (1.45x)[b]	1.64 x 10^{-5} (0.22x)	4.5 x 10^7 (0.7x)	2.2 x 10^{-2} (1.3x)
WT-RdRp	2.0 x 10^9 (1x)	7.5 x 10^{-5} (1x)	6.1 x 10^7 (1x)	1.7 x 10^{-2} (1x)
WT-RdRp + RBV	2.4 x 10^8 (0.12x)	1.6 x 10^{-3} (21x)	1.5 x 10^8 (2.5x)	6.6 x 10^{-3} (0.4x)

[a] Titer in PFU/ml.
[b] All numbers in parentheses are normalized to the WT-RdRp value.
[c] Error frequency was determined by quantifying the frequency of guanidine resistance (PFU/ml in the presence of 1 mM guanidine hydrochloride divided by PFU/ml in the absence of drug).
[d] Viral RNA was extracted from 1 x 10^6 PFU of each virus and quantified by qRT-PCR.
[e] Specific infectivity (PFU/RNA) was calculated by dividing 1 x 10^6 PFU by the number of RNA copies.

CHAPTER THREE

Bacteria-mediated Stabilization of a Panel of Picornaviruses

Introduction

The *Picornaviridae* family includes important human pathogens that can cause a range of diseases such as the common cold, meningitis, hepatitis, and paralysis. The *Picornaviridae* family is diverse and currently includes 80 species in 35 genera. Members of this family are nonenveloped and contain a single-stranded, positive-sense viral genome approximately 7,500 nucleotides in length (Fields Virology, 2013).

Recent studies have shown that bacteria, in particular the gut microbiota, play several important roles during viral infection. Enteric viruses encounter a milieu of microorganisms, including bacteria, both within and outside of the host. It is estimated that these viruses encounter approximately 10^{11} bacteria in the host and are expected to encounter even more in the environment (Sender et al., 2016). Indeed, bacteria enhance infection of several unrelated viruses, including poliovirus, reovirus, rotavirus, MMTV, and norovirus (discussed in “mammalian virus-intestinal microbiota interactions”) (Baldridge et al., 2015; Berger et al., 2017; Jones et al., 2014; Kane et al., 2011; S. K. Kuss et al., 2011; C. M. Robinson et al., 2014; Uchiyama et al., 2014). These “pro-viral” effects are mediated by two known mechanisms: 1) Direct interactions between bacteria and viruses that increased virion stability and attachment to host cells, and 2) indirect interactions between bacteria and the host immune system that modulated immune responses for productive viral infection (Baldridge et al., 2015; Berger et al., 2017; Jones et al., 2014;

Kane et al., 2011; S. K. Kuss et al., 2011; Pfeiffer and Virgin, 2016; C. M. Robinson et al., 2014).

Intriguingly, bacteria and bacterial molecules can inhibit infection with certain viruses. For example, Ichinohe *et al*. demonstrated that certain bacteria promote host immune responses during influenza infection of mice (Ichinohe et al., 2011). More recently, Bandoro *et al*. determined that exposure to the bacterial surface molecule LPS reduced stability of several strains of influenza virus by altering the morphology of the virion envelope (Bandoro and Runstadler, 2017).

Based on the importance of bacterial-viral interactions on viral infection, I sought to determine whether bacteria differentially affect different members of the same viral family, the *Picornaviridae*. I used a panel of four picornaviruses that are spread by the fecal-oral route and represent three separate genera: *Enterovirus* (coxsackievirus B3 (CVB3) and PV), *Kobuvirus* (Aichi virus) and *Cardiovirus* (Mengo virus). I found that a subset of the viral panel were stabilized by bacteria during heat treatment but that all of the picornaviruses tested were stabilized by bacteria during bleach treatment. I also determined that viruses bound to bacteria, indicating that direct interactions may be facilitating viral stabilization of these viruses. This work expands on bacteria-mediated enhancement effects previously observed with PV to other members of the *Picornaviridae* family. Ultimately, this work defines the unique interactions between specific viruses and bacteria which may provide insight into virion environmental stability and transmission.

Materials and methods

Cells and viruses.

HeLa cells were propagated in Dulbecco's modified Eagle's medium (DMEM) supplemented with 10 % calf serum and 1 % penicillin/streptomycin. HeLa cells were used for CVB3, Mengo virus, and PV propagation and quantification of viral titer by plaque assay (Pfeiffer and Kirkegaard, 2003; Rueckert and Pallansch, 1981; Wang and Pfeiffer, 2016). Vero cells were propagated in DMEM supplemented with 10% fetal bovine serum (FBS) and 1 % penicillin/streptomycin. Vero cells were used for Aichi virus propagation and quantification of viral titer by plaque assay. All infections were performed using viruses derived from infectious cDNA clones (the Mengo virus clone was a kind gift from Marco Vignuzzi) (Racaniello and Baltimore, 1981; Sasaki et al., 2001). All viruses were confirmed by Sanger sequencing.

To quantify virus, plaque assay was performed as previously described (Pfeiffer and Kirkegaard, 2003; Rueckert and Pallansch, 1981; Sasaki et al., 2001) Briefly, virus was diluted in phosphate-buffered saline supplemented with 100 µg/mL $CaCl_2$ and 100 µg/mL $MgCl_2$ (PBS+) and added to cells for 30 min at 37°C in presence of 5 % CO_2 to allow for attachment. Agar overlay containing DMEM, supplemented with 20 % calf serum, and 2 % agar was used for CVB3 and PV samples and removed after 48 h. Agar overlay containing DMEM, supplemented with 20 % FBS, and 2 % agar was used for Aichi virus samples and removed after 48 h. Agar overlay containing P5 buffer and 2 % agar was used for Mengo virus samples and removed after 48 h (Rueckert and Pallansch, 1981).

Radiolabeling of picornaviruses was performed as previously described (S. K. Kuss et al., 2011; C. M. Robinson et al., 2014; Wang and Pfeiffer, 2016) . Briefly, viruses were propagated in the presence of ^{35}S-Cysteine/Methionine and were purified using

cesium chloride gradients. Purity of viruses were confirmed by phosphorimaging of radiolabeled capsid proteins on SDS-PAGE, and scintillation count to determine CPM and viable fractions (S. K. Kuss et al., 2011).

Bacterial strains.

Strains of bacteria were from ATCC or from the cecum of mice, as previously described (Erickson et al., 2018). Cultures were inoculated from glycerol stocks in strain-specific nutrient media as previously described (Erickson et al., 2018). Briefly, cultures were grown overnight, bacterial cell pellets were collected and washed in PBS+. After resuspension in 1 mL PBS+, OD_{600} values were obtained by spectrophotometer (Eppendorf BioPhotometer D30) to determine colony forming units (CFUs) needed specific for each assay. Bacteria were UV inactivated prior to use in assays. The amount of bacteria was confirmed by plating on nutrient-specific agar and conditions prior to UV inactivation (Erickson et al., 2018).

Quantifying picornavirus binding to bacterial cells.

Bacterial binding assay was performed as previously described for poliovirus (Erickson et al., 2018). Briefly, approximately 3,000 CPM (approximately 1 x 10^6 PFU) of ^{35}S-radiolabeled virus was mixed with PBS+ or 1 x 10^8 CFU of bacteria and incubated at 37°C in presence of CO_2 for 1 h. After incubation, bacteria was pelleted and washed with PBS+ to remove unbound virus. The amount of CPM (virus bound to bacterial cells) was determined by scintillation counting.

Quantifying effects of bacteria on virion stability.

To determine the effect of bacteria on thermal stability of picornaviruses, 1 x 10^5 PFU of each virus was mixed with PBS+, 1 mg/mL of bacterial surface polysaccharides, or 1 x 10^{10} CFU of bacteria and incubated at 44°C for 4.5 h. The same procedure was followed for elevated temperature assays. After incubation, plaque assays were performed using virus-specific conditions to determine the amount of viable virus before and after heat treatment.

Bleach inactivation assay was performed as previously described for PV, except that a lower concentration of bleach was used here (C. M. Robinson et al., 2014). Briefly, 1 x 10^5 PFU of each virus was mixed with PBS+, 1 mg/mL of bacterial surface polysaccharides, or 1 x 10^8 CFU of bacteria. Samples were incubated at 37°C for 1 h and then added to 0.0001 % fresh bleach for 1 min. Bleach neutralization was done by adding 0.01 % sodium thiosulfate (Sigma). Plaque assays using virus-specific conditions were performed to determine amount of viable virus before and after bleach treatment.

To examine effects of feces on viral stability, feces from four- to ten-week-old male C57BL/6 *PVR-IFNAR -/-* mice were collected and resuspended in PBS+ to a final concentration of 0.0642 mg/μL. Briefly, 1 x 10^5 PFU of virus was mixed with 300 μL of PBS+ or resuspended fecal samples and incubated at 37°C in the presence of 5 % CO_2. Additional samples in PBS+ were placed at 4°C as a control. Samples were taken at designated time points and processed by chloroform extraction as previously described (S. K. Kuss et al., 2011; C. M. Robinson et al., 2014). Plaque assay was performed to determine amount of viable virus before and at designated time points, as described earlier. In Figure 3F, 1 x 10^5 PFU of Mengo virus was mixed with approximately 1 x 10^5

CFU each of *E. coli, P. ruminicola*, and *L. johnsonii* in a total volume of 300 μL and samples were incubated at 37°C. Samples were collected and titers were determined as described above.

Mouse experiments.

Animals were handled according to the Guide for the Care and Use of Laboratory Animals. C57BL/6 *PVR-IFNAR -/-* mice were obtained from S. Koike (Tokyo, Japan) (Ida-Hosonuma et al., 2005). Feces collection was performed at UT Southwestern Medical Center.

Data analysis.

Figures of viral structures were generated using the UCSF Chimera software (http://www.rbvi.ucsf.edu/chimera). The Electron Microscopy Data Bank (EMDB) IDs used for each virus are as follows: Aichi virus (EM-9517), CVB3 (EM-6637) and Saffold virus (EM-3097) to represent their respective genera. The phylogenetic tree was generated using the MEGA7 software and following the Neighbor-Joining Method (Kumar et al., 2016). The optimal tree with the sum of branch length = 2.65 is shown. The tree is drawn to scale, with branch lengths in the same units as those of the evolutionary distances used to infer the phylogenetic tree. The evolutionary distances were computed using the Poisson correction method and are in the units of the number of amino acid substitutions per site. (Tamura et al., 2004). The analysis involved 5 amino acid sequences. All positions containing gaps and missing data were eliminated. There were a total of 766 positions in the final phylogeny tree dataset.

All statistical analyses were performed using the GraphPad Prism Software. Outliers were identified and removed by the ROUT method, Q = 1%. All one way ANOVA tests were performed with Dunnett's multiple comparisons post hoc test. All two-way ANOVA tests were performed with Tukey's post hoc test.

Results

*Panel of viruses from the Picornaviridae family and bacterial strains***.**

Previous studies have indicated that bacteria can reduce the inactivation of poliovirus particles after heat or bleach treatment (S. K. Kuss et al., 2011; C. M. Robinson et al., 2014). In order to investigate whether bacteria stabilize other members of the *Picornaviridae* family from these inactivating conditions, I selected viruses from separate genera and viruses with differences in capsid sequence similarity (Fig. 7 A, B and Table 3). These viruses differ in their capsid structure sequence and topology, which may confer different interactions with bacteria (Fig. 7A). The panel is composed of one virus from the *Kobuvirus* genus (Aichi virus), one virus from the *Cardiovirus* genus (Mengo virus) and three viruses from the Enterovirus genus (PV, CVB3-H3 and CVB3-Nancy). CVB3-Nancy and CVB3-H3 have 98.4% capsid sequence similarity at the amino acid level and were compared to determine whether there are strain-specific differences in bacteria-mediated stabilization (Fig. 7B and Table 3). Additionally, the panel included a PV mutant with a single amino acid change in the VP1 capsid coding region (PV-M132V), that confers enhanced thermal stability in the absence of bacteria (Nguyen Y, 2018 submitted).

I also selected a representative panel of enteric bacteria, and bacterial and non-bacterial molecules (Table 4). I included LPS, which is glycan found on the surface of

Gram negative bacteria. Additionally, I examined two representative Gram-negative bacterial strains (*Escherichia coli* 1470 and *Prevotella ruminicola)*, and two representative Gram-positive bacterial strains (*Bacillus badius* and *Lactobacillus johnsonii).* Our lab previously showed that *E. coli* 1470, *P. ruminicola*, *B. badius* and *L. johnsonii* bind to PV (Erickson et al., 2018), but whether these strains stabilize PV and other picornaviruses was unknown. I also previously showed that non-bacterial compounds, such as bovine albumin serum (BSA) and cellulose, had minimal effects on PV stability and were included in this study as controls (Table 4) (S. K. Kuss et al., 2011; C. M. Robinson et al., 2014).

Specific bacteria enhance stability of a subset of picornaviruses during heat treatment.

To determine whether bacteria enhance stability of picornaviruses, I first examined viral inactivation at elevated temperatures. Picornavirus particles can be inactivated by undergoing premature genome release at a range of temperatures, with faster inactivation at higher temperatures (Plevka et al., 2013; C. M. Robinson et al., 2014; Walter et al., 2012). To increase tractability of my assays, I used relatively high temperatures for the thermal inactivation experiments because inactivation occurs relatively quickly. I first tested viral stability at 44°C for 4.5 h, a condition that I determined inactivates approximately 99% of PV infectivity during incubation in PBS (Fig. 8A). Viruses were mixed with PBS, compounds (BSA, Cellulose or LPS), or bacteria, incubated at 44°C for 4.5 h, and plaque assays were performed to quantify the amount of viable virus remaining. When I incubated PV with any of the bacterial strains or LPS, I observed >50-fold increase in viral stability compared to PBS (Fig. 8A). A similar stabilization was observed for CVB3-H3 and CVB3-Nancy when compared to PBS. Non-bacterial compounds (BSA and

Cellulose) did not stabilize PV or either CVB3 strain. Interestingly, Aichi virus and Mengo virus were very stable in PBS under these conditions. I also tested a recently identified heat-resistant PV mutant, PV-M132V (Nguyen Y, 2018 submitted). Like Aichi virus and Mengo virus, PV-M132V was resistant to heat treatment, and thus incubation with any of the compounds or bacterial strains did not increase stability (Fig. 8A).

I next wanted to determine whether bacteria could increase stability of the heat-stable viruses at temperatures where they become heat labile. First, I increased the temperature in the thermal stability assay to 46°C, and found that similar to the 44°C assay, PV, CVB3-H3, and CVB3-Nancy were stabilized by bacteria (Fig. 8B). Aichi virus, Mengo virus, and PV-M132V were still stable in the 46°C assay and incubation with any of the bacteria compounds or strains did not increase stability. To determine the temperature necessary to inactivate Aichi virus and Mengo virus, I tested viability at temperatures from 46-58°C for 4.5 h. These additional experiments at different temperatures revealed that Aichi virus and Mengo virus were ~99% inactivated when incubated at 50°C or 57°C for 4.5 h, respectively (Fig. 8C-8F). Despite viral inactivation during these conditions, none of the bacterial strains or bacterial polysaccharides could stabilize either of these viruses (Fig. 8D and 8F). Intriguingly, BSA stabilized Aichi virus during incubation at 50°C, indicating this virus may have different requirements for stabilization during heat treatment (Fig. 8D). Overall, these data indicate that bacteria do not stabilize Aichi and Mengo virus during incubation at high temperatures, but that bacterial stabilization of these viruses may be less important given their inherent high stability.

The effect of feces on picornaviruses.

I next wanted to determine whether the viruses in my panel are stabilized in feces. As enteric viruses are transmitted by the fecal-oral route, the potential effects of fecal components on their stability and infection is highly relevant. I previously showed that PV is stabilized in feces from conventional mice (C. M. Robinson et al., 2014). Here, I compared viral stability when viruses were incubated in PBS or feces from conventional mice over the course of several days at 37°C followed by quantification of remaining viable virus by plaque assay. I found that Aichi virus was not stabilized by feces compared to PBS at 37°C after Day 1 (Fig. 9A). Feces only moderately stabilized CVB3-H3 at early timepoints (Fig. 3B). However, CVB3-Nancy and PV were stabilized by feces at later timepoints (see Day 8) (Fig. 9C and 9E). I also demonstrated that PV-M132V was stable during 8 days of incubation at 37°C in both PBS and feces (Nguyen Y, 2018 submitted). Interestingly, Mengo virus exhibited significant inactivation after 4 days at 37°C, but incubation in feces limited this inactivation (Fig. 9D). This result was surprising given the stability of Mengo virus at 46°C for 4.5 h and the lack of bacterial stabilization of Mengo virus at 57°C (Fig. 9B and 9F). However, Mengo virus may have enhanced thermal sensitivity over longer time courses and bacterial effects may be apparent only under these conditions and/or non-bacterial components of feces could affect Mengo virus. When I incubated Mengo virus with mixtures of *E. coli, P. ruminicola*, and *L. johnsonii* at 37°C for several days, Mengo virus was stabilized compared to PBS at 37°C (see dashed line compared to dotted line) (Fig. 9F). These findings indicate that bacteria stabilize Mengo virus during longer exposures to body temperature (37°C) (Fig. 9F). Overall, these

data indicate that several picornaviruses, but not all, are stabilized in feces, which could facilitate transmission.

Bacteria enhance stability of picornaviruses during bleach exposure.

In addition to heat, virions can be inactivated by chlorine bleach via capsid penetration and damage and/or genome release (Alvarez and O'Brien, 1982; Goda et al., 2018; O'Brien and Newman, 1979; Sharp et al., 1975; Wigginton et al., 2012). To determine whether bacteria affect bleach inactivation of viruses, I pre-incubated viruses in PBS, compounds, or bacterial strains for 1 h followed by exposure to dilute bleach (0.0001%) for 1 min, neutralization, and plaque assay to determine the amount of viable virus present. I determined that when pre-incubated in PBS, all viruses lost ~90% of their infectivity (Fig. 10). However, when pre-incubated with LPS or bacterial strains, all viruses were stabilized by at least some of the treatments (Fig. 10). Importantly, pre-incubation of the viruses with BSA or cellulose did not prevent viral inactivation by bleach treatment, indicating that the effects were specific to bacteria and LPS and not just due the presence of additional molecules (Fig. 10). Interestingly, the heat stable PV-M132V mutant virus was inactivated by bleach to the same extent at PV-WT, and bacteria limited bleach inactivation of PV-M132V. These results suggest that thermal inactivation and bleach inactivation occur through separable mechanisms, and that bacteria stabilize virions for both. Overall, these results indicate that bacteria enhance viral stability of fecal-orally transmitted picornaviruses during bleach treatment.

Bacteria bind to a select panel of picornaviruses.

Since bacteria enhanced stability of specific picornaviruses during heat or bleach inactivation, I wanted to determine whether viruses directly interact with bacteria. In particular, I was curious whether bacterial binding efficiencies vary among closely related viruses, such as CVB3-Nancy and CVB3-H3, or between the PV-M132V heat stable mutant and PV-WT. Previously, our lab showed that PV can bind directly to the surface of bacteria (Erickson et al., 2018; S. K. Kuss et al., 2011; C. M. Robinson et al., 2014). ^{35}S-labeled CVB3-Nancy, CVB3-H3, PV-WT, or PV-M132V were incubated with beads, *B. badius*, or *E. coli* for 1 h followed by centrifugation, washing, and scintillation counting the bacterial pellets to quantify viral binding. I determined that PV-WT and PV-M132V bound to both bacterial strains to approximately the same extent (Fig. 11A). This indicates that while the PV-M132V mutant does not require the presence of bacteria for stability during heat treatment, it still binds to bacteria, which could explain why bacteria limit bleach inactivation of PV-M132V (Fig. 10). Additionally, I determined that both CVB3 strains bind to the two bacterial strains tested (Fig. 11B). Interestingly, binding of CVB3-Nancy to *E. coli* was nearly 3-fold higher than CVB3-H3 (Fig. 11B). Overall, these results indicate that multiple picornaviruses bind to bacteria, but with different efficiencies.

Discussion

The *Picornaviridae* family is diverse and includes a large number of medically relevant human pathogens. While it has been shown that bacteria promote infection, co-infection, and transmission of poliovirus, the impact of bacteria on other picornaviruses is unclear (Erickson et al., 2018; S. K. Kuss et al., 2011; C. M. Robinson et al., 2014). Here,

I show that bacteria increase stability of several viruses from the *Picornaviridae* family, likely through direct interactions.

My data show that bacteria-mediated thermal stability can vary among a family of viruses. I determined that certain picornaviruses (*Enterovirus* genus members: CVB3-H3, CVB3-Nancy and PV) are sensitive to heat treatment and that bacteria increase stability of these viruses (Fig. 8 and Fig. 9). I also determined that another picornavirus (*Cardiovirus* genus: Mengo virus) has mixed phenotypes depending on the condition tested. While Mengo virus was very stable at high temperatures during relatively short incubation times (4.5 h) and was not impacted by bacteria under these conditions, it was inactivated after 4 days at 37°C and exposure to feces reduced this inactivation (Fig. 9D). This suggests that Mengo virus may be stabilized by bacteria at physiological temperatures in the host. Finally, I determined that a distantly related picornavirus (*Kobuvirus* genus: Aichi virus) is relatively resistant to high temperature, but is not stabilized by bacteria or bacterial products (Fig. 8 and Fig. 9A). In fact, exposure to feces slightly reduced Aichi virus infectivity (Fig. 9A). Although Aichi virus is transmitted by the fecal-oral route, there are large sequence and structural differences between Aichi and other picornaviruses that may contribute to the different phenotype (Fig. 7 A and B) (C. Sabin et al., 2016; Zhu et al., 2016). Although a member of the *Caliciviridae*, human norovirus can bind to and is stabilized by bacteria that express certain histo-blood group antigens (Li et al., 2015; Miura et al., 2013). Similarly, reovirus (*Reoviridae* family) can be stabilized by exposure to certain bacteria or bacterial surface molecules, but stabilization efficiency and specificity varies among different reovirus strains (Berger et al., 2017).

Taken together, these results indicate that viruses from separate viral families can be stabilized by bacteria, but that not all viruses within a given family share phenotypes.

While picornaviruses vary in bacteria-mediated thermal stabilization, I found that bacteria enhanced viability of all picornaviruses tested during bleach treatment (Fig. 10). Although the PV-M132V mutant was not inactivated at high temperatures, it was inactivated by bleach treatment and bacteria limited this inactivation. Indeed, the PV-M132V virus was determined to bind to bacteria, which could explain stabilization during bleach treatment (Fig. 10). Thus, heat inactivation and bleach inactivation are independent and could have separate requirements for stabilization.

Overall, this study provides insight into the effects of bacteria on a panel of viruses from the same family, the *Picornaviridae*. Understanding the role of bacteria during stabilization and infection of viruses could provide insight into efficient infection within specific hosts (i.e. harboring specific microbiota) as well as between hosts (i.e. environmental bacteria).

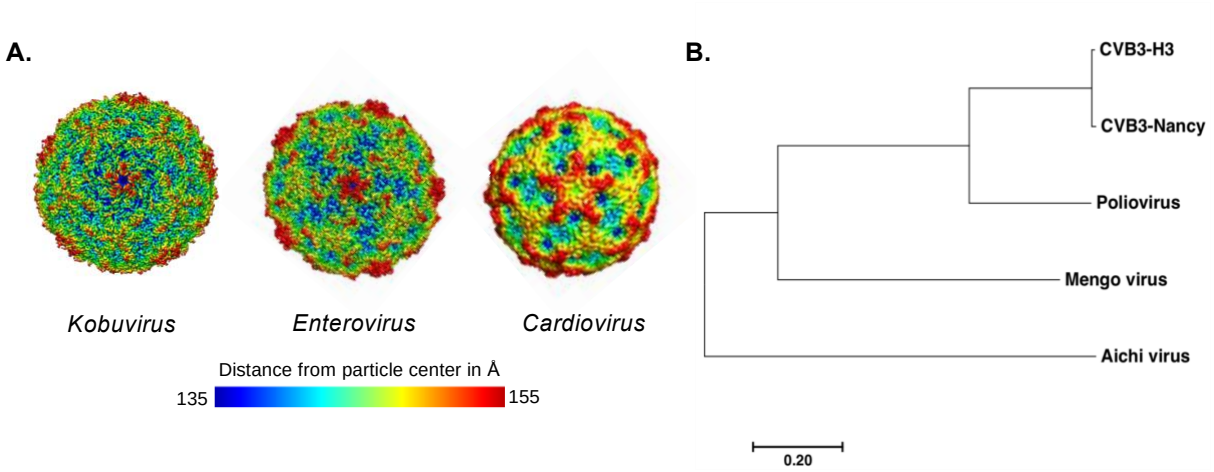

Figure 7. Panel of picornaviruses used in this study. A) Structural models of picornaviruses. Structural comparisons were performed using EMDB ascension numbers for each viral genus and topological distances from the center of the virion calculated from 135 Å (blue) to 155 Å (red), as indicated by the scale bar (C. Sabin et al., 2016). Representative viruses for each genus are Aichi virus (*Kobuvirus*), CVB3 (*Enterovirus*), and Saffold virus (*Cardiovirus*). The Aichi virus structure is at 3.7 Å resolution, CVB3 structure is at 3.9 Å resolution and Saffold virus is at 10.6 Å resolution. Models and distances were generated with UCSF Chimera software. B) Phylogenetic tree of picornaviruses based on the amino acid sequence of the capsid-coding region. The tree was generated using MEGA7 software. The evolutionary history was inferred using the Neighbor-Joining method. The scale bar represents the number of substitutions per site.

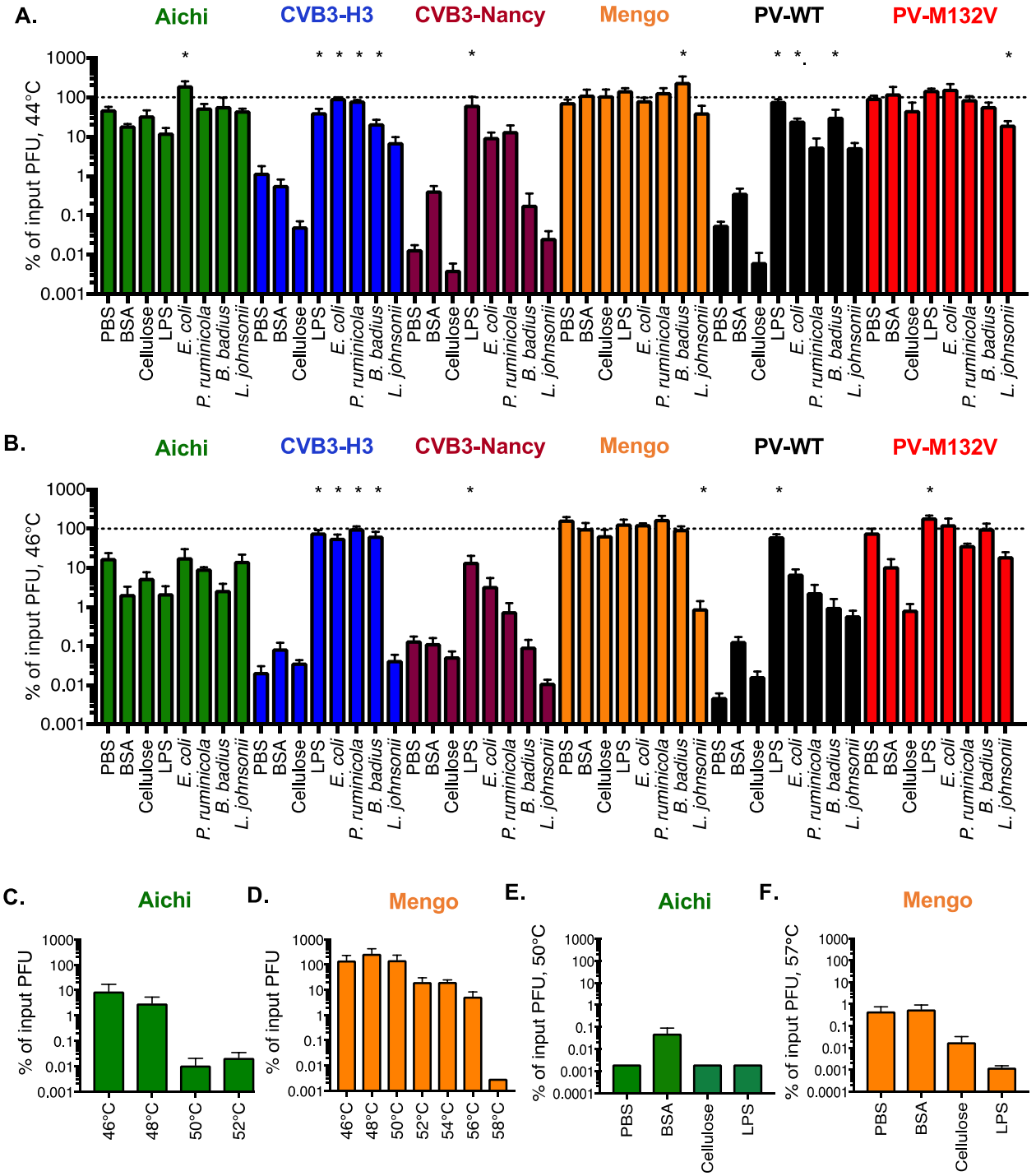

Figure 8. Effects of bacteria and compounds on viral stability at elevated temperatures. Thermal stability assays were performed by incubating 1 x 10^5 PFU viruses in PBS, 1 mg/mL BSA, cellulose, LPS, or 1 x 10^{10} CFU of bacterial strains at various temperatures for 4.5 h. The amount of viable virus following each assay was determined by plaque assay and compared to PBS viral titer at 0 h to determine percent of input PFU. A) 44°C assay. Data are representative of ten to eighteen independent

experiments, n= 4-47. B) 46°C assay. Data are representative of nine to fourteen independent experiments, n= 4-25. C) Incubation of Aichi virus in PBS at various temperatures. Data are representative of two to three independent experiments, n=3-5. D) Incubation of Mengo virus in PBS at various temperatures. Data are representative of one to three independent experiments, n=2-6. E) Aichi virus 50°C assay. Data are representative of two independent experiments, n=4. F) Mengo virus 57°C assay. Data are representative of two experiments, n=4. Bars are shown in SEM. Statistical significance was determined by one-way ANOVA, * = $P<0.05$.

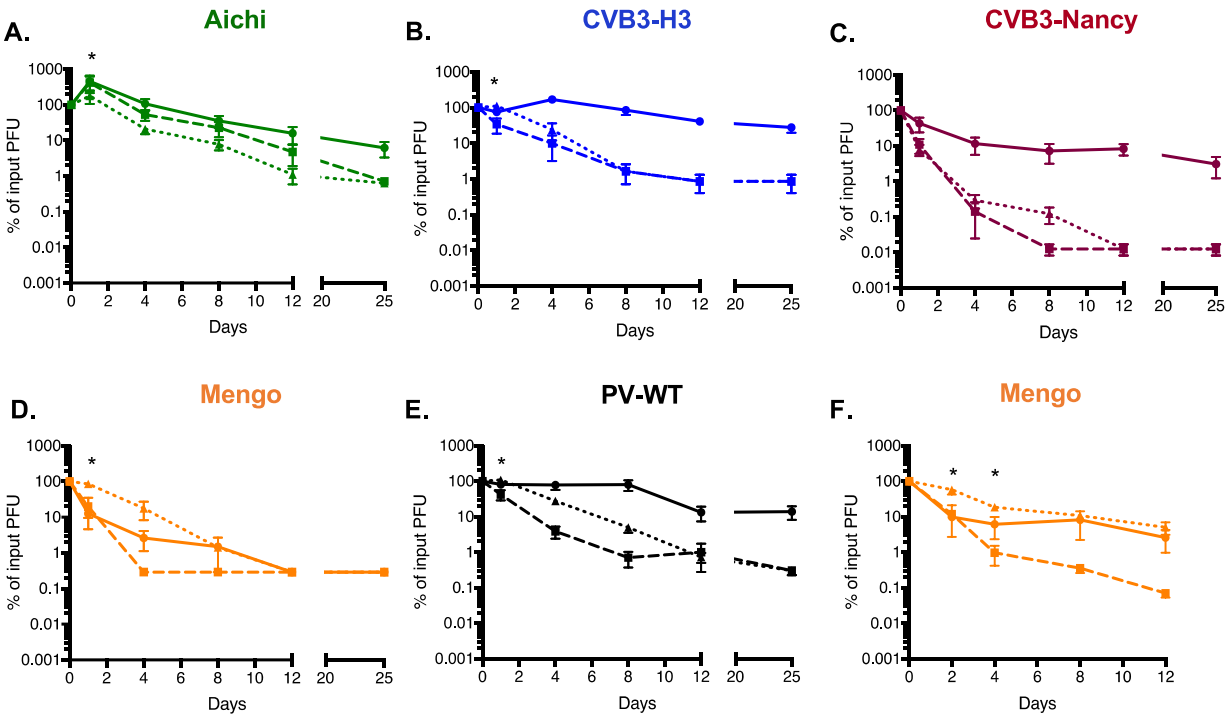

Figure 9. Viral stability in feces. Briefly, 1 x 10^5 PFU of A) Aichi virus, B) CVB3-H3, C) CVB3 Nancy, D) Mengo virus E) PV was incubated with PBS or a slurry of feces from mice and incubated at 37°C (PBS, dashed lines; Feces, dotted lines) or 4°C (PBS, solid lines). Data are representative of two to three experiments, n = 4-5. In F) 1 x 10^5 PFU of Mengo virus was incubated with PBS or a mixture of bacteria and incubated at 37°C (PBS, dashed lines; Bacteria, dotted lines) or 4°C (PBS, solid lines). Data are representative of two independent experiments, n = 4. Samples were taken at designated time points and processed prior to plaque assay for quantification of viable virus. Bars are shown in SEM. Statistical significance between PBS and feces or bacteria at 37°C was determined by two-way ANOVA, * = P<0.05.

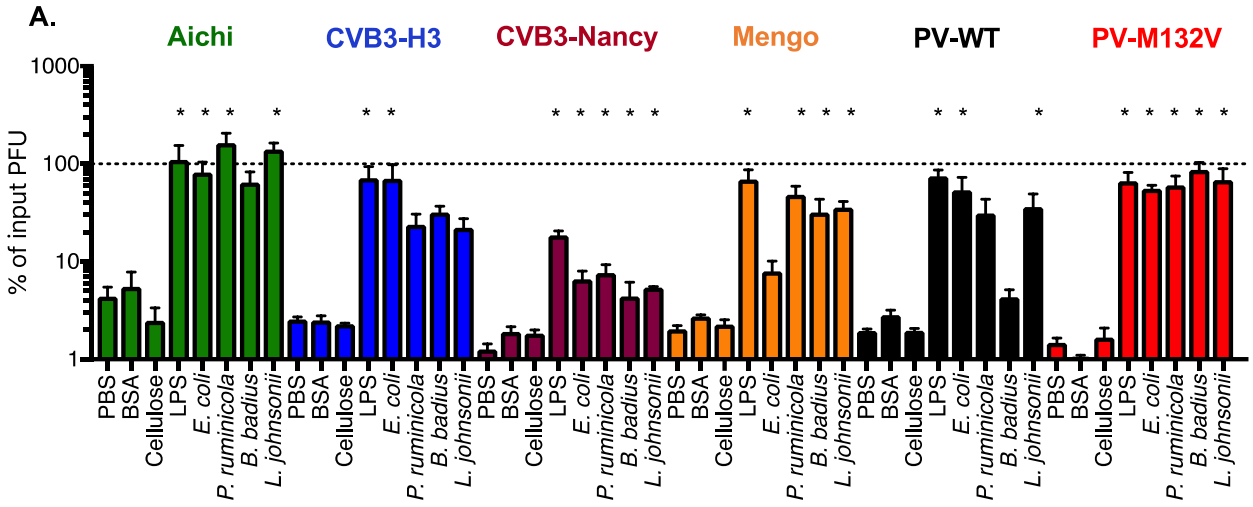

Figure 10. Effects of bacteria on viral stability during bleach treatment. 1 x 10^5 PFU viruses were incubated individually in PBS, 1 mg/mL BSA, cellulose, LPS, or 1 x 10^8 CFU of bacterial strains at 37°C for 1 h. After incubation, samples were treated with 0.0001% bleach for 1 minute and neutralized with sodium thiolsulfate. Amount of viable virus was determined by plaque assay and compared to PBS viral titer at 0 h to determine % of input PFU. Data are representative of seven to twenty independent experiments, n = 4-40. Bars are shown in SEM. Statistical significance was determined by one-way ANOVA, * = P<0.05.

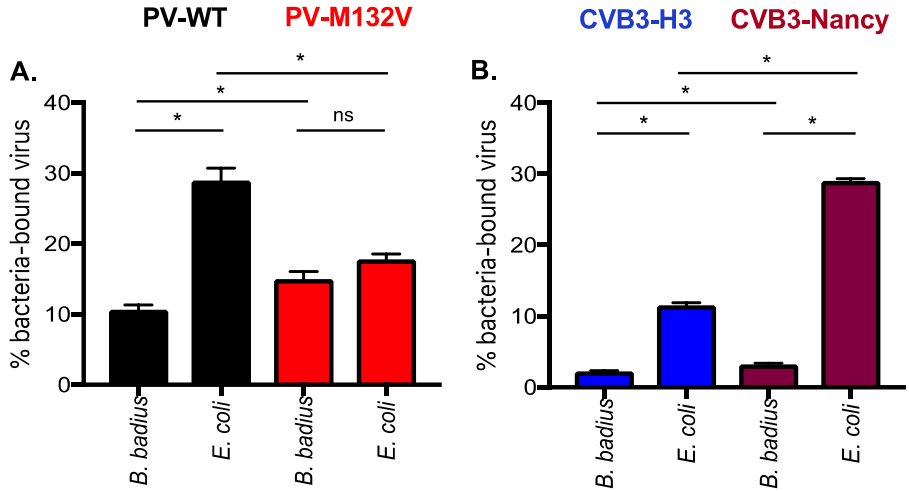

Figure 11. Picornaviruses bind to bacteria. ^{35}S-labeled viruses (3,000 CPM/ approximately 1 x 10^6 PFU) were incubated with 1 x 10^8 CFU of bacteria for 1 h at 37°C. After incubation, samples were spun down and washed to remove unbound virus. Bound virus was quantified by scintillation counting. Data are representative of two independent experiments, n=3-4. Bars are shown in SEM. * = *P*<0.05, based on student's T test. n.s., not significant.

Table 3. Percent sequence identity between panel of picornaviruses

Capsid Amino Acid Sequence Similarity (%)

Family and genus	**Virus**	Aichi virus	Mengo virus	CVB3-H3	CVB3-Nancy	Poliovirus
Picornaviridae						
Kobuvirus	Aichi virus	100.0	28.6	23.3	23.3	24.3
Cardiovirus	Mengo virus		100.0	30.0	29.8	29.0
Enterovirus	CVB3-H3			100.0	98.6	54.4
	CVB3-Nancy				100.0	54.2
	Poliovirus					100.0

Table 4. List of reagents and bacterial strains used in this study.

Name	Gram Status	Phylum	Source
Bovine Albumin Serum (BSA)			Fischer Scientific
Cellulose			Sigma
Lipopolysaccharide			Sigma (0127:B8)
Escherichia coli 1470	Gram-negative	Proteobacteria	Mouse cecum
Prevotella ruminicola	Gram-negative	Bacteroidetes	ATCC 19189
Bacillus badius	Gram-positive	Firmicutes	Mouse cecum
Lactobacillus johnsonii	Gram-positive	Firmicutes	Mouse cecum

CHAPTER FOUR

Discussion and Concluding Remarks

RNA viruses are of pressing concern due to the large variety of diseases that they cause in humans. One reason for this is their vast genetic diversity that allows these viruses to propagate in new hosts and also surpass restrictive barriers in the environment and within the host. The studies described in this dissertation focused on multiple factors that affect RNA enteric virus infection in an effort to provide insight on mechanisms of viral evolution, stabilization and transmission.

In Chapter 2, I described how RNA viruses could form virion aggregates and that this form of infectious unit could lead to the simultaneous co-infection and subsequent plaque formation of mammalian cells (Fig. 4 and Fig. 12). Additionally, several other mechanisms may facilitate co-infection of RNA viruses. Apart from aggregation, viruses packaged within vesicle-like structures and viruses bound to intestinal bacteria facilitate co-infection (Fig. 12). These mechanisms could also affect infection kinetics within the host. Factors, such as aggregation and the presence of bacteria, could potentially facilitate co-infection during the initial round of infection. Moreover, cell-to-cell transmission by vesicle-like structures could facilitate the transport of several viral particles and/or genomes from infected cells to neighboring cells at or following the initial round of infection.

I further showed that heavily mutagenized viruses had an increase in co-infection and subsequent plaque formation (Fig. 5). This finding was particularly intriguing since it is possible that specific genetic processes, such as recombination and complementation, could result in the resurrection of otherwise defective viral genomes. This, of course,

could have serious implications for viral diversity and evolution. Future studies regarding the genetic consequences of these separate co-infection mechanisms would be an intriguing area of interest to determine their impact on viral diversity. Overall, the studies described here highlight the existence of novel mechanisms that influence co-infection of RNA viruses and potentially promote viral evolution.

In Chapter 3, I described how different RNA viruses from the same viral family, the *Picornaviridae*, are affected by bacteria during select inactivating conditions. Our lab provided seminal evidence that bacteria play an important role during infection of poliovirus, but whether other members of the same viral family exploit bacteria to the same extent had not been explored until this work. To examine this question, I used a panel of picornaviruses that represent members from three separate genera. In performing this work, I also established Aichi virus and Mengo virus for use as new viral systems to test in the lab. This panel of picornaviruses have varying capsid sequence similarities and the surface capsid for these viruses could likely be the interacting component with bacteria and other environmental compounds (Fig. 7). Despite large differences among viruses at the capsid level (for example, Aichi and Mengo viruses displaying ~30% sequence similarity to poliovirus), all viruses in the panel were stabilized by bacteria during bleach treatment, indicating a possible universal interacting component with bacteria that could be mediating stabilization during this specific insult (Fig. 10).

On the other hand, specific bacterial strains appeared to stabilize specific picornaviruses during treatment at elevated temperatures (Fig. 8). Intriguingly, Aichi virus and Mengo virus were stable at these elevated temperatures. When heat-labile, bacteria and their compounds still did not stabilize Aichi or Mengo virus, but bacteria did appear

to stabilize Mengo virus only during prolonged exposure at physiological temperatures (Fig. 8E, 8F and 9F). These data could indicate “viral preferences” of bacteria during specific inactivating conditions.

The stabilization effects of bacteria are likely directly mediated since I determined that all of the viruses tested could bind to bacteria. Intriguingly, CVB3-H3 and CVB3-Nancy had large differences in binding (Fig 11B). The observation that CVB3-H3 and CVB3-Nancy had large differences in binding to *E. coli* but similar binding to *B. badius* could be a continued area of study to further delineate specific capsid residues required for binding that vary between the two strains (which share ~98% similarity). Given these new findings, the exact viral residue(s) necessary for interaction with bacteria has yet to be determined and warrants further investigation for these, and other, viruses.

Overall, the work described in this dissertation has shed light on unique and universal mechanisms that influence mammalian RNA viruses during transmission and infection.

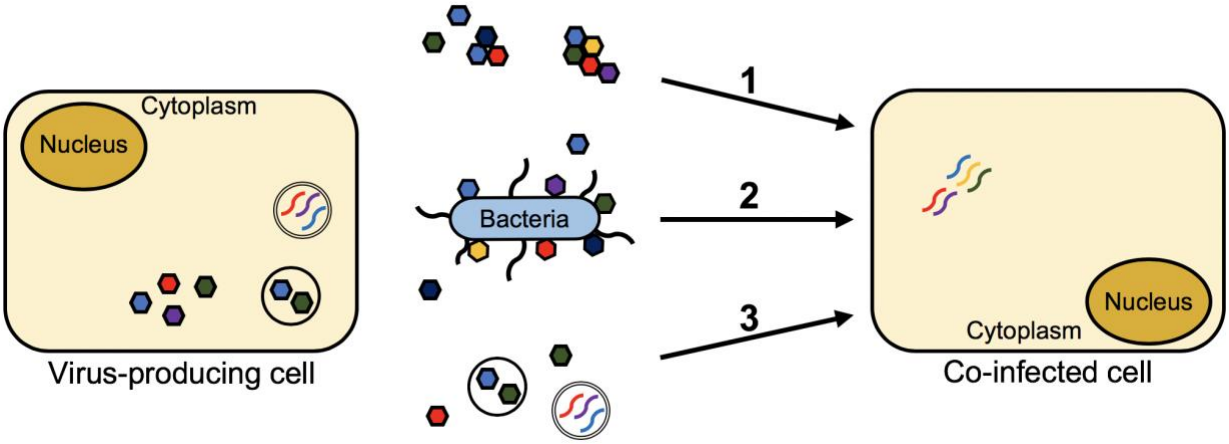

Figure 12. Mechanisms of viral co-infection. Viral co-infection of mammalian cells can be induced by 1) Virion aggregates, 2) Bacteria bound by several viral particles, and 3) Release of viral particles or viral genomes within membrane vesicles. Genetically distinct viruses are depicted as multi-colored hexagons (virions) or curved lines (genomes).

BIBLIOGRAPHY

Alvarez, M. E., & O'Brien, R. T. (1982). Effects of chlorine concentration on the structure of poliovirus. *Appl Environ Microbiol, 43*(1), 237-239.

Arita, M., Zhu, S. L., Yoshida, H., Yoneyama, T., Miyamura, T., & Shimizu, H. (2005). A Sabin 3-derived poliovirus recombinant contained a sequence homologous with indigenous human enterovirus species C in the viral polymerase coding region. *J Virol, 79*(20), 12650-12657.

Arnold, J. J., Vignuzzi, M., Stone, J. K., Andino, R., & Cameron, C. E. (2005). Remote site control of an active site fidelity checkpoint in a viral RNA-dependent RNA polymerase. *J Biol Chem, 280*(27), 25706-25716.

Baldridge, M. T., Nice, T. J., McCune, B. T., Yokoyama, C. C., Kambal, A., Wheadon, M., . . . Virgin, H. W. (2015). Commensal microbes and interferon-lambda determine persistence of enteric murine norovirus infection. *Science, 347*(6219), 266-269. doi:10.1126/science.1258025

Bandoro, C., & Runstadler, J. A. (2017). Bacterial Lipopolysaccharide Destabilizes Influenza Viruses. *mSphere, 2*(5). doi:10.1128/mSphere.00267-17

Bergelson, J. M., Cunningham, J. A., Droguett, G., Kurt-Jones, E. A., Krithivas, A., Hong, J. S., . . . Finberg, R. W. (1997). Isolation of a common receptor for Coxsackie B viruses and adenoviruses 2 and 5. *Science, 275*(5304), 1320-1323.

Berger, A. K., Yi, H., Kearns, D. B., & Mainou, B. A. (2017). Bacteria and bacterial envelope components enhance mammalian reovirus thermostability. *PLoS Pathog, 13*(12), e1006768. doi:10.1371/journal.ppat.1006768

Bird, S. W., & Kirkegaard, K. (2015). Escape of non-enveloped virus from intact cells. *Virology, 479-480*, 444-449. doi:10.1016/j.virol.2015.03.044

Bird, S. W., Maynard, N. D., Covert, M. W., & Kirkegaard, K. (2014). Nonlytic viral spread enhanced by autophagy components. *Proc Natl Acad Sci U S A, 111*(36), 13081-13086. doi:10.1073/pnas.1401437111

Bookout, A. L., Cummins, C. L., Mangelsdorf, D. J., Pesola, J. M., & Kramer, M. F. (2006). High-throughput real-time quantitative reverse transcription PCR. *Curr Protoc Mol Biol, Chapter 15*, Unit 15 18. doi:10.1002/0471142727.mb1508s73

Burness, A. T., & Pardoe, I. U. (1983). A sialoglycopeptide from human erythrocytes with receptor-like properties for encephalomyocarditis and influenza viruses. *J Gen Virol, 64*(Pt 5), 1137-1148. doi:10.1099/0022-1317-64-5-1137

Carocci, M., & Bakkali-Kassimi, L. (2012). The encephalomyocarditis virus. *Virulence, 3*(4), 351-367. doi:10.4161/viru.20573

Cash, H. L., Whitham, C. V., Behrendt, C. L., & Hooper, L. V. (2006). Symbiotic bacteria direct expression of an intestinal bactericidal lectin. *Science, 313*(5790), 1126-1130. doi:10.1126/science.1127119

Chebath, J., Benech, P., Revel, M., & Vigneron, M. (1987). Constitutive expression of (2'-5') oligo A synthetase confers resistance to picornavirus infection. *Nature, 330*(6148), 587-588. doi:10.1038/330587a0

Chen, Y. H., Du, W., Hagemeijer, M. C., Takvorian, P. M., Pau, C., Cali, A., . . . Altan-Bonnet, N. (2015). Phosphatidylserine vesicles enable efficient en bloc transmission of enteroviruses. *Cell, 160*(4), 619-630. doi:10.1016/j.cell.2015.01.032

Cherkasova, E. A., Korotkova, E. A., Yakovenko, M. L., Ivanova, O. E., Eremeeva, T. P., Chumakov, K. M., & Agol, V. I. (2002). Long-term circulation of vaccine-derived poliovirus that causes paralytic disease. *J Virol, 76*(13), 6791-6799.

Combe, M., Garijo, R., Geller, R., Cuevas, J. M., & Sanjuan, R. (2015). Single-Cell Analysis of RNA Virus Infection Identifies Multiple Genetically Diverse Viral Genomes within Single Infectious Units. *Cell Host Microbe, 18*(4), 424-432. doi:10.1016/j.chom.2015.09.009

Crotty, S., Cameron, C. E., & Andino, R. (2001). RNA virus error catastrophe: direct molecular test by using ribavirin. *Proc Natl Acad Sci U S A, 98*(12), 6895-6900.

Cuervo, N. S., Guillot, S., Romanenkova, N., Combiescu, M., Aubert-Combiescu, A., Seghier, M., . . . Delpeyroux, F. (2001). Genomic features of intertypic recombinant sabin poliovirus strains excreted by primary vaccinees. *J Virol, 75*(13), 5740-5751.

Dahourou, G., Guillot, S., Le Gall, O., & Crainic, R. (2002). Genetic recombination in wild-type poliovirus. *J Gen Virol, 83*(Pt 12), 3103-3110. doi:10.1099/0022-1317-83-12-3103

Dalldorf, G., & Sickles, G. M. (1948). An Unidentified, Filtrable Agent Isolated From the Feces of Children With Paralysis. *Science, 108*(2794), 61-62. doi:10.1126/science.108.2794.61

Dalldorf, G., Sickles, G. M., & et al. (1949). A virus recovered from the feces of poliomyelitis patients pathogenic for suckling mice. *J Exp Med, 89*(6), 567-582.

Dick, G. W., Best, A. M., & et al. (1948). Mengo encephalomyelitis; a hitherto unknown virus affecting man. *Lancet, 2*(6521), 286-289.

Dolan, P. T., Whitfield, Z. J., & Andino, R. (2018). Mechanisms and Concepts in RNA Virus Population Dynamics and Evolution. *Annu Rev Virol*. doi:10.1146/annurev-virology-101416-041718

Domingo, E., & Holland, J. J. (1997). RNA virus mutations and fitness for survival. *Annu Rev Microbiol, 51*, 151-178. doi:10.1146/annurev.micro.51.1.151

Domingo, E., Martinez-Salas, E., Sobrino, F., de la Torre, J. C., Portela, A., Ortin, J., . . . et al. (1985). The quasispecies (extremely heterogeneous) nature of viral RNA genome populations: biological relevance--a review. *Gene, 40*(1), 1-8.

Dominguez-Bello, M. G., Costello, E. K., Contreras, M., Magris, M., Hidalgo, G., Fierer, N., & Knight, R. (2010). Delivery mode shapes the acquisition and structure of the initial microbiota across multiple body habitats in newborns. *Proc Natl Acad Sci U S A, 107*(26), 11971-11975. doi:10.1073/pnas.1002601107

Drake, J. W. (1993). Rates of spontaneous mutation among RNA viruses. *Proc Natl Acad Sci U S A, 90*(9), 4171-4175.

Dreux, M., Garaigorta, U., Boyd, B., Decembre, E., Chung, J., Whitten-Bauer, C., . . . Chisari, F. V. (2012). Short-range exosomal transfer of viral RNA from infected cells to plasmacytoid dendritic cells triggers innate immunity. *Cell Host Microbe, 12*(4), 558-570. doi:10.1016/j.chom.2012.08.010

Duarte, E., Clarke, D., Moya, A., Domingo, E., & Holland, J. (1992). Rapid fitness losses in mammalian RNA virus clones due to Muller's ratchet. *Proc Natl Acad Sci U S A, 89*(13), 6015-6019.

Dulbecco, R., & Vogt, M. (1953). Some problems of animal virology as studied by the plaque technique. *Cold Spring Harb Symp Quant Biol, 18*, 273-279.

Eckburg, P. B., Bik, E. M., Bernstein, C. N., Purdom, E., Dethlefsen, L., Sargent, M., . . . Relman, D. A. (2005). Diversity of the human intestinal microbial flora. *Science, 308*(5728), 1635-1638. doi:10.1126/science.1110591

Erickson, A. K., Jesudhasan, P. R., Mayer, M. J., Narbad, A., Winter, S. E., & Pfeiffer, J. K. (2018). Bacteria Facilitate Enteric Virus Co-infection of Mammalian Cells and Promote Genetic Recombination. *Cell Host Microbe, 23*(1), 77-88 e75. doi:10.1016/j.chom.2017.11.007

Feng, Z., Hensley, L., McKnight, K. L., Hu, F., Madden, V., Ping, L., . . . Lemon, S. M. (2013). A pathogenic picornavirus acquires an envelope by hijacking cellular membranes. *Nature, 496*(7445), 367-371. doi:10.1038/nature12029

Fields Virology. (2013). *6th Edition*. Philadelphia, PA, USA: Lippincott Williams & Wilkins.

Floyd, R., & Sharp, D. G. (1977). Aggregation of poliovirus and reovirus by dilution in water. *Appl Environ Microbiol, 33*(1), 159-167.

Floyd, R., & Sharp, D. G. (1978). Viral aggregation: effects of salts on the aggregation of poliovirus and reovirus at low pH. *Appl Environ Microbiol, 35*(6), 1084-1094.

Floyd, R., & Sharp, D. G. (1979). Viral aggregation: buffer effects in the aggregation of poliovirus and reovirus at low and high pH. *Appl Environ Microbiol, 38*(3), 395-401.

Furione, M., Guillot, S., Otelea, D., Balanant, J., Candrea, A., & Crainic, R. (1993). Polioviruses with natural recombinant genomes isolated from vaccine-associated paralytic poliomyelitis. *Virology, 196*(1), 199-208.

Garmaroudi, F. S., Marchant, D., Hendry, R., Luo, H., Yang, D., Ye, X., . . . McManus, B. M. (2015). Coxsackievirus B3 replication and pathogenesis. *Future Microbiol, 10*(4), 629-653. doi:10.2217/fmb.15.5

Ghabrial, S. A., & Suzuki, N. (2009). Viruses of plant pathogenic fungi. *Annu Rev Phytopathol, 47*, 353-384. doi:10.1146/annurev-phyto-080508-081932

Goda, H., Ikeda, K., Nishide, M., Nagao, T., & Koyama, A. H. (2018). Characterization of Virucidal Activities of Chlorous Acid. *Jpn J Infect Dis*. doi:10.7883/yoken.JJID.2018.089

Hafenstein, S., Bowman, V. D., Chipman, P. R., Bator Kelly, C. M., Lin, F., Medof, M. E., & Rossmann, M. G. (2007). Interaction of decay-accelerating factor with coxsackievirus B3. *J Virol, 81*(23), 12927-12935. doi:10.1128/JVI.00931-07

Holmblat, B., Jegouic, S., Muslin, C., Blondel, B., Joffret, M. L., & Delpeyroux, F. (2014). Nonhomologous recombination between defective poliovirus and coxsackievirus genomes suggests a new model of genetic plasticity for picornaviruses. *MBio, 5*(4), e01119-01114. doi:10.1128/mBio.01119-14

Honda, K., & Littman, D. R. (2012). The microbiome in infectious disease and inflammation. *Annu Rev Immunol, 30*, 759-795. doi:10.1146/annurev-immunol-020711-074937

Huber, S. A. (1994). VCAM-1 is a receptor for encephalomyocarditis virus on murine vascular endothelial cells. *J Virol, 68*(6), 3453-3458.

Huizinga, J. D., & Lammers, W. J. (2009). Gut peristalsis is governed by a multitude of cooperating mechanisms. *Am J Physiol Gastrointest Liver Physiol, 296*(1), G1-8. doi:10.1152/ajpgi.90380.2008

Ibarra, K. D., & Pfeiffer, J. K. (2009). Reduced ribavirin antiviral efficacy via nucleoside transporter-mediated drug resistance. *J Virol, 83*(9), 4538-4547. doi:JVI.02280-08 [pii]

10.1128/JVI.02280-08
Ichinohe, T., Pang, I. K., Kumamoto, Y., Peaper, D. R., Ho, J. H., Murray, T. S., & Iwasaki, A. (2011). Microbiota regulates immune defense against respiratory tract influenza A virus infection. *Proc Natl Acad Sci U S A, 108*(13), 5354-5359. doi:10.1073/pnas.1019378108
Ida-Hosonuma, M., Iwasaki, T., Yoshikawa, T., Nagata, N., Sato, Y., Sata, T., . . . Koike, S. (2005). The alpha/beta interferon response controls tissue tropism and pathogenicity of poliovirus. *J Virol, 79*(7), 4460-4469. doi:10.1128/JVI.79.7.4460-4469.2005
Ida-Hosonuma, M., Sasaki, Y., Toyoda, H., Nomoto, A., Gotoh, O., Yonekawa, H., & Koike, S. (2003). Host range of poliovirus is restricted to simians because of a rapid sequence change of the poliovirus receptor gene during evolution. *Arch Virol, 148*(1), 29-44. doi:10.1007/s00705-002-0910-7
Johansson, M. E., Phillipson, M., Petersson, J., Velcich, A., Holm, L., & Hansson, G. C. (2008). The inner of the two Muc2 mucin-dependent mucus layers in colon is devoid of bacteria. *Proc Natl Acad Sci U S A, 105*(39), 15064-15069. doi:10.1073/pnas.0803124105
Jones, M. K., Watanabe, M., Zhu, S., Graves, C. L., Keyes, L. R., Grau, K. R., . . . Karst, S. M. (2014). Enteric bacteria promote human and mouse norovirus infection of B cells. *Science, 346*(6210), 755-759. doi:10.1126/science.1257147
Kane, M., Case, L. K., Kopaskie, K., Kozlova, A., MacDearmid, C., Chervonsky, A. V., & Golovkina, T. V. (2011). Successful transmission of a retrovirus depends on the commensal microbiota. *Science, 334*(6053), 245-249. doi:10.1126/science.1210718
Kew, O., Morris-Glasgow, V., Landaverde, M., Burns, C., Shaw, J., Garib, Z., . . . de Quadros, C. (2002). Outbreak of poliomyelitis in Hispaniola associated with circulating type 1 vaccine-derived poliovirus. *Science, 296*(5566), 356-359. doi:10.1126/science.1068284
Kirkegaard, K., & Baltimore, D. (1986). The mechanism of RNA recombination in poliovirus. *Cell, 47*(3), 433-443.
Kitajima, M., & Gerba, C. P. (2015). Aichi virus 1: environmental occurrence and behavior. *Pathogens, 4*(2), 256-268. doi:10.3390/pathogens4020256
Koike, S., Taya, C., Kurata, T., Abe, S., Ise, I., Yonekawa, H., & Nomoto, A. (1991). Transgenic mice susceptible to poliovirus. *Proc Natl Acad Sci U S A, 88*(3), 951-955.
Kumar, S., Stecher, G., & Tamura, K. (2016). MEGA7: Molecular Evolutionary Genetics Analysis Version 7.0 for Bigger Datasets. *Mol Biol Evol, 33*(7), 1870-1874. doi:10.1093/molbev/msw054
Kuss, S., Etheredge, C., & Pfeiffer, J. (2008). Mulitple Host Barriers Restrict Poliovirus Trafficking in Mice. *PLoS Pathog, 4*(6), e1000082.
Kuss, S. K., Best, G. T., Etheredge, C. A., Pruijssers, A. J., Frierson, J. M., Hooper, L. V., . . . Pfeiffer, J. K. (2011). Intestinal microbiota promote enteric virus replication and systemic pathogenesis *Science, 334*(6053), 249-252.
Kuss, S. K., Best, G. T., Etheredge, C. A., Pruijssers, A. J., Frierson, J. M., Hooper, L. V., . . . Pfeiffer, J. K. (2011). Intestinal microbiota promote enteric virus replication and

systemic pathogenesis. *Science, 334*(6053), 249-252. doi:10.1126/science.1211057

Ladner, J. T., Wiley, M. R., Beitzel, B., Auguste, A. J., Dupuis, A. P., 2nd, Lindquist, M. E., . . . Palacios, G. (2016). A Multicomponent Animal Virus Isolated from Mosquitoes. *Cell Host Microbe, 20*(3), 357-367. doi:10.1016/j.chom.2016.07.011

Lancaster, K. Z., & Pfeiffer, J. K. (2010). Limited Trafficking of a Neurotropic Virus Through Inefficient Retrograde Axonal Transport and the Type I Interferon Response. *PLoS Pathog, 6*(3), e1000791.

Landsteiner, K. P., E. (1909). Übertragung der Poliomyelitis acuta auf Affen. . *Zeitschrift für Immunitatsforschung*.

Leveque, N., & Semler, B. L. (2015). A 21st century perspective of poliovirus replication. *PLoS Pathog, 11*(6), e1004825. doi:10.1371/journal.ppat.1004825

Li, D., Breiman, A., le Pendu, J., & Uyttendaele, M. (2015). Binding to histo-blood group antigen-expressing bacteria protects human norovirus from acute heat stress. *Front Microbiol, 6*, 659. doi:10.3389/fmicb.2015.00659

Liu, H. M., Zheng, D. P., Zhang, L. B., Oberste, M. S., Pallansch, M. A., & Kew, O. M. (2000). Molecular evolution of a type 1 wild-vaccine poliovirus recombinant during widespread circulation in China. *J Virol, 74*(23), 11153-11161.

Lodder, W. J., Rutjes, S. A., Takumi, K., & de Roda Husman, A. M. (2013). Aichi virus in sewage and surface water, the Netherlands. *Emerg Infect Dis, 19*(8), 1222-1230. doi:10.3201/eid1908.130312

Longatti, A., Boyd, B., & Chisari, F. V. (2015). Virion-independent transfer of replication-competent hepatitis C virus RNA between permissive cells. *J Virol, 89*(5), 2956-2961. doi:10.1128/JVI.02721-14

Luethy, L. N., Erickson, A. K., Jesudhasan, P. R., Ikizler, M., Dermody, T. S., & Pfeiffer, J. K. (2016). Comparison of three neurotropic viruses reveals differences in viral dissemination to the central nervous system. *Virology, 487*, 1-10. doi:10.1016/j.virol.2015.09.019

Macpherson, A. J., & Uhr, T. (2004). Induction of protective IgA by intestinal dendritic cells carrying commensal bacteria. *Science, 303*(5664), 1662-1665. doi:10.1126/science.1091334

Mendelsohn, C., Johnson, B., Lionetti, K. A., Nobis, P., Wimmer, E., & Racaniello, V. R. (1986). Transformation of a human poliovirus receptor gene into mouse cells. *Proc Natl Acad Sci U S A, 83*(20), 7845-7849.

Mendelsohn, C. L., Wimmer, E., & Racaniello, V. R. (1989). Cellular receptor for poliovirus: molecular cloning, nucleotide sequence, and expression of a new member of the immunoglobulin superfamily. *Cell, 56*(5), 855-865.

Miura, T., Sano, D., Suenaga, A., Yoshimura, T., Fuzawa, M., Nakagomi, T., . . . Okabe, S. (2013). Histo-blood group antigen-like substances of human enteric bacteria as specific adsorbents for human noroviruses. *J Virol, 87*(17), 9441-9451. doi:10.1128/JVI.01060-13

Muller, H. J. (1964). The Relation of Recombination to Mutational Advance. *Mutat Res, 106*, 2-9.

Nathanson, N. (2008). The pathogenesis of poliomyelitis: what we don't know. *Adv Virus Res, 71*, 1-50. doi:10.1016/S0065-3527(08)00001-8

Nguyen Y, J. P., Aguilera ER, Pfeiffer JK. (2018 submitted). Characterization of a thermal stable poliovirus mutant reveals distinct mechanisms of virion stabilization.

O'Brien, R. T., & Newman, J. (1979). Structural and compositional changes associated with chlorine inactivation of polioviruses. *Appl Environ Microbiol, 38*(6), 1034-1039.

Ohka, S., Igarashi, H., Nagata, N., Sakai, M., Koike, S., Nochi, T., . . . Nomoto, A. (2007). Establishment of a poliovirus oral infection system in human poliovirus receptor-expressing transgenic mice that are deficient in alpha/beta interferon receptor. *J Virol, 81*(15), 7902-7912. doi:10.1128/JVI.02675-06

Ouzilou, L., Caliot, E., Pelletier, I., Prevost, M. C., Pringault, E., & Colbere-Garapin, F. (2002). Poliovirus transcytosis through M-like cells. *J Gen Virol, 83*(Pt 9), 2177-2182. doi:10.1099/0022-1317-83-9-2177

Peterson, L. W., & Artis, D. (2014). Intestinal epithelial cells: regulators of barrier function and immune homeostasis. *Nat Rev Immunol, 14*(3), 141-153. doi:10.1038/nri3608

Pfeiffer, J. K., & Kirkegaard, K. (2003). A single mutation in poliovirus RNA-dependent RNA polymerase confers resistance to mutagenic nucleotide analogs via increased fidelity. *Proc Natl Acad Sci U S A, 100*(12), 7289-7294.

Pfeiffer, J. K., & Kirkegaard, K. (2005). Increased fidelity reduces poliovirus fitness and virulence under selective pressure in mice. *PLoS Pathog, 1*(2), e11. doi:10.1371/journal.ppat.0010011

Pfeiffer, J. K., & Virgin, H. W. (2016). Viral immunity. Transkingdom control of viral infection and immunity in the mammalian intestine. *Science, 351*(6270). doi:10.1126/science.aad5872

Plevka, P., Perera, R., Yap, M. L., Cardosa, J., Kuhn, R. J., & Rossmann, M. G. (2013). Structure of human enterovirus 71 in complex with a capsid-binding inhibitor. *Proc Natl Acad Sci U S A, 110*(14), 5463-5467. doi:10.1073/pnas.1222379110

Racaniello, V. R. (2006). One hundred years of poliovirus pathogenesis. *Virology, 344*(1), 9-16. doi:10.1016/j.virol.2005.09.015

Racaniello, V. R., & Baltimore, D. (1981). Molecular cloning of poliovirus cDNA and determination of the complete nucleotide sequence of the viral genome. *Proc Natl Acad Sci U S A, 78*(8), 4887-4891.

Ramakrishnaiah, V., Thumann, C., Fofana, I., Habersetzer, F., Pan, Q., de Ruiter, P. E., . . . van der Laan, L. J. (2013). Exosome-mediated transmission of hepatitis C virus between human hepatoma Huh7.5 cells. *Proc Natl Acad Sci U S A, 110*(32), 13109-13113. doi:10.1073/pnas.1221899110

Rao, A. L. (2006). Genome packaging by spherical plant RNA viruses. *Annu Rev Phytopathol, 44*, 61-87. doi:10.1146/annurev.phyto.44.070505.143334

Ren, R., & Racaniello, V. R. (1992). Human poliovirus receptor gene expression and poliovirus tissue tropism in transgenic mice. *J Virol, 66*(1), 296-304.

Ren, R. B., Costantini, F., Gorgacz, E. J., Lee, J. J., & Racaniello, V. R. (1990). Transgenic mice expressing a human poliovirus receptor: a new model for poliomyelitis. *Cell, 63*(2), 353-362.

Robinson, C. M., Jesudhasan, P. R., & Pfeiffer, J. K. (2014). Bacterial lipopolysaccharide binding enhances virion stability and promotes environmental fitness of an enteric virus. *Cell Host Microbe, 15*(1), 36-46. doi:10.1016/j.chom.2013.12.004

Robinson, C. M., Wang, Y., & Pfeiffer, J. K. (2017). Sex-Dependent Intestinal Replication of an Enteric Virus. *J Virol, 91*(7). doi:10.1128/JVI.02101-16

Robinson, S. M., Tsueng, G., Sin, J., Mangale, V., Rahawi, S., McIntyre, L. L., . . . Feuer, R. (2014). Coxsackievirus B exits the host cell in shed microvesicles displaying autophagosomal markers. *PLoS Pathog, 10*(4), e1004045. doi:10.1371/journal.ppat.1004045

Rossmann, M. G., He, Y., & Kuhn, R. J. (2002). Picornavirus-receptor interactions. *Trends Microbiol, 10*(7), 324-331.

Rueckert, R. R., & Pallansch, M. A. (1981). Preparation and characterization of encephalomyocarditis (EMC) virus. *Methods Enzymol, 78*(Pt A), 315-325.

Sabin, A. B. (1959). Present position of immunization against poliomyelitis with live virus vaccines. *Br Med J, 1*(5123), 663-680.

Sabin, C., Fuzik, T., Skubnik, K., Palkova, L., Lindberg, A. M., & Plevka, P. (2016). Structure of Aichi virus 1 and its empty particle: clues towards kobuvirus genome release mechanism. *J Virol*. doi:10.1128/JVI.01601-16

Salk, J. E., Krech, U., Youngner, J. S., Bennett, B. L., Lewis, L. J., & Bazeley, P. L. (1954). Formaldehyde treatment and safety testing of experimental poliomyelitis vaccines. *Am J Public Health Nations Health, 44*(5), 563-570.

Santiana, M., Ghosh, S., Ho, B. A., Rajasekaran, V., Du, W. L., Mutsafi, Y., . . . Altan-Bonnet, N. (2018). Vesicle-Cloaked Virus Clusters Are Optimal Units for Inter-organismal Viral Transmission. *Cell Host Microbe, 24*(2), 208-220 e208. doi:10.1016/j.chom.2018.07.006

Sarnow, P., Bernstein, H., & Baltimore, D. (1986). A poliovirus temperature-sensitive RNA synthesis mutant located in a noncoding region of the genome. *Proc Natl Acad Sci USA, 83*, 571-575.

Sasaki, J., Kusuhara, Y., Maeno, Y., Kobayashi, N., Yamashita, T., Sakae, K., . . . Taniguchi, K. (2001). Construction of an infectious cDNA clone of Aichi virus (a new member of the family Picornaviridae) and mutational analysis of a stem-loop structure at the 5' end of the genome. *J Virol, 75*(17), 8021-8030.

Schaffer, J., Beamer, P. R., Trexler, P. C., Breidenbach, G., & Walcher, D. N. (1963). Response of germ-free animals to experimental virus monocontamination. I. Observation on Coxsackie B virus. *Proc Soc Exp Biol Med, 112*, 561-564.

Selinka, H. C., Wolde, A., Pasch, A., Klingel, K., Schnorr, J. J., Kupper, J. H., . . . Kandolf, R. (2002). Comparative analysis of two coxsackievirus B3 strains: putative influence of virus-receptor interactions on pathogenesis. *J Med Virol, 67*(2), 224-233. doi:10.1002/jmv.2211

Sender, R., Fuchs, S., & Milo, R. (2016). Revised Estimates for the Number of Human and Bacteria Cells in the Body. *PLoS Biol, 14*(8), e1002533. doi:10.1371/journal.pbio.1002533

Sergiescu, D., Aubert-Combiescu, A., & Crainic, R. (1969). Recombination between guanidine-resistant and dextran sulfate-resistant mutants of type 1 poliovirus. *J Virol, 3*(3), 326-330.

Shabram, P., & Aguilar-Cordova, E. (2000). Multiplicity of infection/multiplicity of confusion. *Mol Ther, 2*(5), 420-421. doi:10.1006/mthe.2000.0212

Shafren, D. R., Bates, R. C., Agrez, M. V., Herd, R. L., Burns, G. F., & Barry, R. D. (1995). Coxsackieviruses B1, B3, and B5 use decay accelerating factor as a receptor for cell attachment. *J Virol, 69*(6), 3873-3877.

Shah, V. A., Chong, C. Y., Chan, K. P., Ng, W., & Ling, A. E. (2003). Clinical characteristics of an outbreak of hand, foot and mouth disease in Singapore. *Ann Acad Med Singapore, 32*(3), 381-387.

Sharp, D. G., & Dunlap, R. C. (1966). Multiplicity reactivation of vaccinia virus in the cells of the chorioallantoic membrane. *Proc Soc Exp Biol Med, 123*(1), 111-114.

Sharp, D. G., Floyd, R., & Johnson, J. D. (1975). Nature of the surviving plaque-forming unit of reovirus in water containing bromine. *Appl Microbiol, 29*(1), 94-101.

Sicinski, P., Rowinski, J., Warchol, J. B., Jarzabek, Z., Gut, W., Szczygiel, B., . . . Koch, G. (1990). Poliovirus type 1 enters the human host through intestinal M cells. *Gastroenterology, 98*(1), 56-58.

Silhavy, T. J., Kahne, D., & Walker, S. (2010). The bacterial cell envelope. *Cold Spring Harb Perspect Biol, 2*(5), a000414. doi:10.1101/cshperspect.a000414

Simmonds, P., Bukh, J., Combet, C., Deleage, G., Enomoto, N., Feinstone, S., . . . Widell, A. (2005). Consensus proposals for a unified system of nomenclature of hepatitis C virus genotypes. *Hepatology, 42*(4), 962-973.

Suzuki, K., Meek, B., Doi, Y., Muramatsu, M., Chiba, T., Honjo, T., & Fagarasan, S. (2004). Aberrant expansion of segmented filamentous bacteria in IgA-deficient gut. *Proc Natl Acad Sci U S A, 101*(7), 1981-1986. doi:10.1073/pnas.0307317101

Tamura, K., Nei, M., & Kumar, S. (2004). Prospects for inferring very large phylogenies by using the neighbor-joining method. *Proc Natl Acad Sci U S A, 101*(30), 11030-11035. doi:10.1073/pnas.0404206101

Tershak, D. R. (1982). Inhibition of poliovirus polymerase by guanidine in vitro. *J Virol, 41*(1), 313-318.

Teterina, N. L., Levenson, E. A., & Ehrenfeld, E. (2010). Viable polioviruses that encode 2A proteins with fluorescent protein tags. *J Virol, 84*(3), 1477-1488. doi:10.1128/JVI.01578-09

Turnbaugh, P. J., Hamady, M., Yatsunenko, T., Cantarel, B. L., Duncan, A., Ley, R. E., . . . Gordon, J. I. (2009). A core gut microbiome in obese and lean twins. *Nature, 457*(7228), 480-484. doi:10.1038/nature07540

Uchiyama, R., Chassaing, B., Zhang, B., & Gewirtz, A. T. (2014). Antibiotic treatment suppresses rotavirus infection and enhances specific humoral immunity. *J Infect Dis, 210*(2), 171-182. doi:10.1093/infdis/jiu037

Vaishnava, S., Yamamoto, M., Severson, K. M., Ruhn, K. A., Yu, X., Koren, O., . . . Hooper, L. V. (2011). The antibacterial lectin RegIIIgamma promotes the spatial segregation of microbiota and host in the intestine. *Science, 334*(6053), 255-258. doi:10.1126/science.1209791

Valtanen, S., Roivainen, M., Piirainen, L., Stenvik, M., & Hovi, T. (2000). Poliovirus-specific intestinal antibody responses coincide with decline of poliovirus excretion. *J Infect Dis, 182*(1), 1-5. doi:10.1086/315684

Veckenstedt, A. (1974). Pathogenicity of mengo virus to mice. I. Virological studies. *Acta Virol, 18*(6), 501-507.

Vignuzzi, M., Stone, J. K., & Andino, R. (2005). Ribavirin and lethal mutagenesis of poliovirus: molecular mechanisms, resistance and biological implications. *Virus Res, 107*(2), 173-181.

Vignuzzi, M., Stone, J. K., Arnold, J. J., Cameron, C. E., & Andino, R. (2006). Quasispecies diversity determines pathogenesis through cooperative interactions in a viral population. *Nature, 439*(7074), 344-348. doi:10.1038/nature04388

Wallis, C., & Melnick, J. L. (1967). Virus aggregation as the cause of the non-neutralizable persistent fraction. *J Virol, 1*(3), 478-488.

Walter, T. S., Ren, J., Tuthill, T. J., Rowlands, D. J., Stuart, D. I., & Fry, E. E. (2012). A plate-based high-throughput assay for virus stability and vaccine formulation. *J Virol Methods, 185*(1), 166-170. doi:10.1016/j.jviromet.2012.06.014

Wang, Y., & Pfeiffer, J. K. (2016). Emergence of a Large-Plaque Variant in Mice Infected with Coxsackievirus B3. *MBio, 7*(2), e00119. doi:10.1128/mBio.00119-16

Ward, C. D., Stokes, M. A., & Flanegan, J. B. (1988). Direct measurement of the poliovirus RNA polymerase error frequency in vitro. *J Virol, 62*(2), 558-562.

Wigginton, K. R., Pecson, B. M., Sigstam, T., Bosshard, F., & Kohn, T. (2012). Virus inactivation mechanisms: impact of disinfectants on virus function and structural integrity. *Environ Sci Technol, 46*(21), 12069-12078. doi:10.1021/es3029473

Xiao, Y., Dolan, P. T., Goldstein, E. F., Li, M., Farkov, M., Brodsky, L., & Andino, R. (2017). Poliovirus intrahost evolution is required to overcome tissue-specific innate immune responses. *Nat Commun, 8*(1), 375. doi:10.1038/s41467-017-00354-5

Yamashita, T., Kobayashi, S., Sakae, K., Nakata, S., Chiba, S., Ishihara, Y., & Isomura, S. (1991). Isolation of cytopathic small round viruses with BS-C-1 cells from patients with gastroenteritis. *J Infect Dis, 164*(5), 954-957.

Yamashita, T., Sakae, K., Tsuzuki, H., Suzuki, Y., Ishikawa, N., Takeda, N., . . . Yamazaki, S. (1998). Complete nucleotide sequence and genetic organization of Aichi virus, a distinct member of the Picornaviridae associated with acute gastroenteritis in humans. *J Virol, 72*(10), 8408-8412.

Young, D. C., & Sharp, D. G. (1977). Poliovirus aggregates and their survival in water. *Appl Environ Microbiol, 33*(1), 168-177.

Yuste, E., Sanchez-Palomino, S., Casado, C., Domingo, E., & Lopez-Galindez, C. (1999). Drastic fitness loss in human immunodeficiency virus type 1 upon serial bottleneck events. *J Virol, 73*(4), 2745-2751.

Zautner, A. E., Korner, U., Henke, A., Badorff, C., & Schmidtke, M. (2003). Heparan sulfates and coxsackievirus-adenovirus receptor: each one mediates coxsackievirus B3 PD infection. *J Virol, 77*(18), 10071-10077.

Zhu, L., Wang, X., Ren, J., Kotecha, A., Walter, T. S., Yuan, S., . . . Stuart, D. I. (2016). Structure of human Aichi virus and implications for receptor binding. *Nat Microbiol, 1*(11), 16150. doi:10.1038/nmicrobiol.2016.150